

**SURFACE CHARACTERIZATION OF POLYVINYLIDENE
FLUORIDE (PVDF) IN ITS APPLICATION AS AN ACTUATOR**

A Thesis

by

SAIKUMAR MANI

Submitted to the Office of Graduate Studies of
Texas A&M University
in partial fulfillment of the requirements for the degree of

MASTER OF SCIENCE

May 2007

Major Subject: Mechanical Engineering

**SURFACE CHARACTERIZATION OF POLYVINYLIDENE
FLUORIDE (PVDF) IN ITS APPLICATION AS AN ACTUATOR**

A Thesis

by

SAIKUMAR MANI

Submitted to the Office of Graduate Studies of
Texas A&M University
in partial fulfillment of the requirements for the degree of

MASTER OF SCIENCE

Approved by:

Chair of the Committee, Hong Liang
Committee Members, Zoubeida Ounaies
Xinghang Zhang
Head of the Department, Dennis O'Neal

May 2007

Major Subject: Mechanical Engineering

ABSTRACT

Surface Characterization of Polyvinylidene Fluoride (PVDF) in Its Application as an Actuator. (May 2007)

Saikumar Mani, B.E., Anna University

Chair of Advisory Committee: Dr. Hong Liang

Polyvinylidene Fluoride (PVDF) is a common piezoelectric polymer. It is widely utilized because of its advantageous mechanical, chemical, and electromechanical properties. An interesting application for its properties lies in using it as an actuator, specifically for a microgripper device. The microgripper has many applications such as surgeries, microassembly, and micromanipulation. The friction force is an important criterion that greatly affects the gripping. This research studies the frictional behavior of the PVDF and effects of applied electrical potential. Approaches include tribological investigation of the polymer associated with surface properties. The surface characterization was conducted using a profilometer and an Atomic Force Microscope (AFM). In addition, the application of a PVDF material as a microgripper is addressed along with the design of the gripper.

It was found that the friction could be turned-on and off because of external applied electrical potential. Such behavior was associated with the microstructure, where dipoles were aligned in an electrical field. Such active-friction has not been reported in the past. This work opens new areas of research in fundamental friction that benefits the design and development of small devices such as a microgripper.

DEDICATION

Dedicated to the memory of my late father, who always inspires me to success and who instilled in me the value of education and hard work and to my mother who has been a constant source of support through tough times and who showers affection on me always.

ACKNOWLEDGEMENTS

My heartfelt thanks are due to my advisor, Dr. Liang who believes in me and who has guided me to scale heights. I wish to thank her for her constant support, guidance and encouragement. I also wish to thank her for being an example of working relentlessly to achieve goals and for instilling self initiative in me. I wish to thank Dr. Ounaies for imparting invaluable knowledge in certain areas of the project and for helping me immensely during my work. I wish to thank Dr. Zhang for agreeing to be part of my committee and for encouraging me. Thanks are also due to Dr. Hung for supporting me and imparting knowledge about an interesting application.

This work would not be possible without the invaluable help and contributions by Dr. Ricardo Perez, Hyungoo Lee and Sumanth Banda. Thanks are also due to Taekwon Jee and Atheer Almasri for imparting knowledge during the initial stages of this project.

Thanks are due to the group members in the surface science laboratory who have been very supportive during this work and who have helped me understand the importance of team work.

Thanks are due to the sponsorship of the NSF (grant number IIS-0515930), the Texas Engineering Experiment Station, and Texas A&M University.

I wish to take this opportunity to thank all my friends, old and new, for putting up with me and for sticking with me and constantly inspiring me to achieve goals.

Finally many thanks to my parents, brother and other family members for all their love and support and to God for making my dreams come true.

TABLE OF CONTENTS

	Page
ABSTRACT	iii
DEDICATION	iv
ACKNOWLEDGEMENTS	v
TABLE OF CONTENTS	vi
LIST OF FIGURES.....	viii
LIST OF TABLES	x
1. INTRODUCTION.....	1
1.1 Historical Background.....	1
1.2 Concept of Piezoelectricity	3
1.3 Piezoelectric Polymers	7
1.4 PVDF.....	9
1.5 Actuators	13
1.6 Microgripper.....	14
1.7 Motivation	16
2. THEORIES AND PRINCIPLES	18
2.1 Friction Characterization.....	18
2.2 Surface Characterization	21
2.2.1 Atomic Force Microscopy.....	21
2.2.2 Surface Profilometer	24
2.3 Actuation	25
2.4 Microgripper Design	28
3. EXPERIMENTAL	30
3.1 Materials.....	30
3.1.1 Synthesis of PVDF Films.....	30
3.1.2 Electroding	34
3.1.3 Sample Materials.....	35
3.2 Friction Testing	36
3.3 Surface Characterization	39
3.3.1 Surface Profilometry	39
3.3.2 AFM Characterization.....	40
3.4 Actuation	41
3.5 Design of the Microgripper	43
4. RESULTS.....	44

	Page
4.1 Friction Characterization.....	44
4.2 Surface Characterization	49
4.2.1 Surface Profiling	49
4.2.2 AFM Characterization.....	51
4.3 Actuation	53
4.4 Microgripper Design	55
5. DISCUSSIONS	58
5.1 Frictional Behavior.....	58
5.2 Effects of Surface Roughness on Friction.....	60
5.3 Piezoelectricity Dominated Frictional Behavior	61
5.4 Effects of Stress on Piezoelectricity.....	63
5.5 Actuation Tests.....	65
5.6 Microgripper Design	66
6. CONCLUSIONS	68
6.1 Summary	68
6.2 Suggested Future Research	69
REFERENCES	70
VITA	77

LIST OF FIGURES

	Page
Fig. 1 Tensor directions for defining constitutive relations	4
Fig. 2 Structure of PVDF	10
Fig. 3 β phase of PVDF	11
Fig. 4 Tactile microgripper, adapted from the design by Kim et al.	16
Fig. 5 Tribometer setup	18
Fig. 6 Pin on disk configuration	19
Fig. 7 Linearizing the plot of μ vs. time in the software TriboX	20
Fig. 8 Schematics of an AFM setup	22
Fig. 9 AFM setup showing the TESE configuration	23
Fig. 10 Surface profilometer TR 200 and the probes used.....	24
Fig. 11 Sample profile plot from the profilometer	25
Fig. 12 Actuation of a polymer	26
Fig. 13 Effect of application of external electric field on PVDF	27
Fig. 14 BiSlide system	28
Fig. 15 Solution casting of PVDF	31
Fig. 16 Procedure to make PVDF Films	33
Fig. 17 Hummer sputtering system	34
Fig. 18 Sample for testing	36
Fig. 19 Experimental setup for tribotesting.....	37
Fig. 20 Interface for tribotesting	37
Fig. 21 TriboX software interface	39
Fig. 22 Actuator configurations	42
Fig. 23 Plot of speed of reciprocation against coefficient of friction.....	45
Fig. 24 Plot of applied normal force against coefficient of friction	45
Fig. 25 Comparison of sample A and B based on μ vs. voltage	47
Fig. 26 Comparison of sample A and C based on μ vs. voltage	48

	Page
Fig. 27 Surface roughness versus voltage for the various samples.....	50
Fig. 28 AFM probe displacement with applied voltage	51
Fig. 29 AFM Images with the application of 5V	52
Fig. 30 Deflection characterization of PVDF.....	54
Fig. 31 Design of the microgripper attachment.....	55
Fig. 32 Line diagram of the microgripper attachment	57
Fig. 33 Hertzian contact stress	64

LIST OF TABLES

	Page
Table 1 Description of the samples used.....	35
Table 2 Inverting voltage tests for samples A, B and C.....	48
Table 3 Reverse polarity tests	49
Table 4 Surface roughness of the samples at different voltages	50

1. INTRODUCTION

Piezoelectricity by definition is the electric charge generated in a material when mechanical pressure is applied to it. The opposite effect is the inverse piezoelectricity which leads to change in the shape of a material when an electric charge is applied to it. These two effects are the foundation of the phenomenon of piezoelectricity.

Polyvinylidene Fluoride (PVDF) is a commercially available, piezoelectric polymer. It is widely utilized due to its advantageous mechanical, chemical, and electromechanical properties.

There has been significant research and a wide range of applications of piezoelectric materials as actuators. Nevertheless, the surface characterization, and effects of externally applied electric fields have yet to be further investigated.

The thesis includes 6 Sections. After a brief introduction in Section 1, an outline of the various theories and principles is described in Section 2. Following this, the experimental procedures and results are covered in Section 3 and 4. Discussion of the results and conclusion is talked about after these in Sections 5 and 6 respectively.

1.1 Historical Background

Historically piezoelectricity was first discovered in 1880 by the Curie brothers, Jacques and Pierre, who announced their experiments at the session of the Académie des Sciences in Paris [1, 2]. They worked with materials like Rochelle salt, quartz and tourmaline and studied how mechanical energy was converted into electrical energy with a high efficiency. For a long period of time it remained an unclear phenomenon and remained a scientific curiosity rather than a practical application.

This thesis follows the style of ASME Journal of Tribology.

In 1916, a Frenchman Paul Langevin devised the first major application by developing an ultrasonic submarine detector. The detector consisted of a transducer, made of thin quartz crystals carefully glued between two steel plates, and a hydrophone to detect the returned echo. By emitting a high-frequency chirp from the transducer, and measuring the amount of time it takes to hear an echo from the sound waves bouncing off an object, one can calculate the distance to that object. The principle behind this was with the inverse piezoelectric effect bouncing the sonar off the object in the water and recaptured by the quartz plate [3]. Later on, the Bell Telephone Laboratories developed multi-channel telephones using the quartz crystals as wave filters [4]. In 1930's and 1940's, it entered the period when the crystal phonographs were used in microphones.

The first synthetic substance used as a piezoelectric was Barium Titanate, BaTiO_3 . It has piezoelectric capabilities comparable to Rochelle salt; the voltages developed under pressure are approximately of the same magnitude, and the size changes in the crystal when voltage is applied are similar [5]. The BaTiO_3 has many advantages over the natural piezoelectric crystals such as positive temperature coefficient and higher permittivity.

Other man-made piezoelectrics like lead metaniobate and lead titanate zirconate (PZT) were discovered in the following years, each offering still greater improvements in piezoelectric characteristics and physical properties [6].

In 1968, synthetic quartz crystals started becoming available and this helped reduce the dependency on the natural crystals [4].

In 1969, Kawai [7] discovered that a strong piezoelectric effect could be induced in Polyvinylidene Fluoride (PVDF) by applying an electric field. He showed that poled thin films exhibited a large piezoelectric coefficient.

In 1971, Bergman et al. [8] and Wada et al. [9] discovered that PVDF films polarized this way also exhibited pyroelectricity with pyroelectric figures of merit comparable to crystalline pyroelectric detectors.

In 1989, Barsky et al. [10] developed a PVDF sensor-based feedback manipulating microgripper system. In 2003, Kim et al. [11] worked and developed a novel design for a PVDF microgripper. This system also used the force feedback controlled gripping based on the piezoelectric polymer. In 1990's, a number of these microgripper applications were developed due to the trend in technological advancement in microassembly and microrobotics.

Currently Piezoelectric crystals are used in a number of ways, the most important being high voltage sources (cigarette lighters), sensors (microphones), actuators (loudspeakers), frequency standards (quartz clocks), piezoelectric motors (cameras) and ultrasonic transducers (medical purposes) [3, 4, 12].

1.2 Concept of Piezoelectricity

The word “piezo” means press from the greek word “piezin” and hence piezoelectricity is the ability of certain crystals to generate a voltage in response to applied mechanical stress. That is, when mechanical pressure is applied to one of these materials, the crystalline structure produces a voltage proportional to the pressure. Conversely, when an electric field is applied, the structure changes shape producing dimensional changes in the material [1]. The deformation, about 0.1% of the original dimension in PZT, is of the order of nanometers, but nevertheless finds useful applications such as the production and detection of sound, generation of high voltages, electronic frequency generation, and ultra fine focusing of optical assemblies [3, 13, 14].

Many other materials exhibit the piezoelectric effect, including quartz analogue crystals like berlinite (AlPO_4) and gallium orthophosphate (GaPO_4), ceramics with perovskite or

tungsten-bronze structures (BaTiO_3 , SrTiO_3 , PbZrTiO_3 , KNbO_3 , LiNbO_3 , LiTaO_3 , BiFeO_3 , Na_xWO_3 , $\text{Ba}_2\text{NaNb}_5\text{O}_{15}$, $\text{Pb}_2\text{KNb}_5\text{O}_{15}$) [15]. Polymeric materials like rubber, wool, hair, wood fiber, and silk exhibit piezoelectricity to some extent. The polymer polyvinylidene fluoride, PVDF, exhibits piezoelectricity several times larger than quartz [16].

Polarization is defined as the separation of the center of the positive and negative electric charges, making one side of the crystal positive and the opposite side negative. The electrical response of piezo-materials is a function of both stress (T) applied to the electrode area and the mechanical strain (S) that the material experiences [4].

The constitutive relations of piezoelectricity in materials can be derived using a tensor notation. The directions are depicted in the figure 1 below.

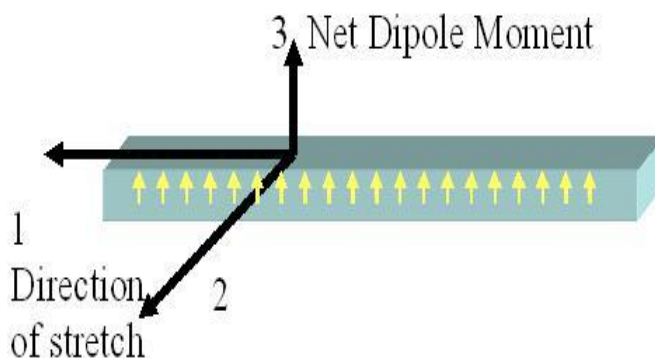


Fig. 1 Tensor directions for defining constitutive relations

The stretch direction is axis 1. Axis 2 is orthogonal to this and axis 3 is the polarization axis, along which is the net dipole moment. Axes 4, 5 and 6 represent the shear planes and are perpendicular to the other 3 axes 1, 2 and 3 respectively and are not depicted in this figure.

Piezoelectricity is the combined effect of the electrical behavior of the material $D=\epsilon^*E$ and Hooke's Law $S=s^*T$, where D is volumetric charge density, ϵ is permittivity and E is electric field strength, S is strain, s is compliance and T is stress.

These may be combined into so-called coupled equations, of which the strain-charge form is:

$$\{S\}=[s^E]\{T\}+[d_t]\{E\}$$

$$\{D\}=[d]\{T\}+[\epsilon^T]\{E\}$$

where the superscript E indicates a zero, or constant, electric field; the superscript T indicates a zero, or constant, stress field; and the subscript t stands for transposition of a matrix.

The strain-charge form may also be written as:

$$\begin{bmatrix} S_1 \\ S_2 \\ S_3 \\ S_4 \\ S_5 \\ S_6 \end{bmatrix} = \begin{bmatrix} s_{11}^E & s_{12}^E & s_{13}^E & 0 & 0 & 0 \\ s_{12}^E & s_{11}^E & s_{13}^E & 0 & 0 & 0 \\ s_{13}^E & s_{13}^E & s_{33}^E & 0 & 0 & 0 \\ 0 & 0 & 0 & s_{44}^E & 0 & 0 \\ 0 & 0 & 0 & 0 & s_{44}^E & 0 \\ 0 & 0 & 0 & 0 & 0 & s_{66}^E = 2(s_{11}^E - s_{12}^E) \end{bmatrix} \begin{bmatrix} T_1 \\ T_2 \\ T_3 \\ T_4 \\ T_5 \\ T_6 \end{bmatrix} + \begin{bmatrix} 0 & 0 & d_{31} \\ 0 & 0 & d_{31} \\ 0 & 0 & d_{33} \\ 0 & d_{15} & 0 \\ d_{15} & 0 & 0 \\ 0 & 0 & 0 \end{bmatrix} \begin{bmatrix} E_1 \\ E_2 \\ E_3 \end{bmatrix}$$

$$\begin{bmatrix} D_1 \\ D_2 \\ D_3 \end{bmatrix} = \begin{bmatrix} 0 & 0 & 0 & 0 & d_{15} & 0 \\ 0 & 0 & 0 & d_{15} & 0 & 0 \\ d_{31} & d_{31} & d_{33} & 0 & 0 & 0 \end{bmatrix} \begin{bmatrix} T_1 \\ T_2 \\ T_3 \\ T_4 \\ T_5 \\ T_6 \end{bmatrix} + \begin{bmatrix} \epsilon_{11} & 0 & 0 \\ 0 & \epsilon_{11} & 0 \\ 0 & 0 & \epsilon_{33} \end{bmatrix} \begin{bmatrix} E_1 \\ E_2 \\ E_3 \end{bmatrix}$$

The coupling of these two equations gives the piezoelectric strain constant d and the material compliance s and the permittivity ϵ .

The resulting piezoelectric coefficient d_{33} , which relates the applied electric field in the thickness direction to the strain in the same direction, is negative for PVDF and this has to be considered for our testing. Since the net polarization exists only in the 3 direction no change in the charge is expected on the 1 and 2 directions when uniaxial stress is applied. This is because the 3 surface is the one that is electroded and the d_{3j} components of the piezoelectric tensor are the most frequently reported [17].

Tensile stress is considered positive so that positive stress in the 3 direction causes an increase in the thickness of the film, a decrease in the polarization and hence a negative coefficient. Similarly a tension in the 1 or 2 directions causes a positive coefficient.

Other piezoelectric properties are the piezoelectric voltage constant g , stress constant d and strain constant h .

$$g = \left(\frac{\partial E}{\partial X} \right)_{D=0}$$

$$d = \left(\frac{\partial D}{\partial x} \right)_{E=0}$$

$$h = \left(\frac{\partial E}{\partial x} \right)_{D=0}$$

The piezoelectric coefficients d that relate the charge developed on the film surface to the stress exerted on the material are commonly known for these polymers and are smaller than those the piezoceramic materials, and also the dielectric constants are small [18]. This in turn makes the voltage generated per unit stress larger and this is represented by the g coefficients.

The piezoelectric response is able to stiffen the material due to the increased strain through stress and polarization.

$$X_{polarization} = eE$$

where e is the electrical displacement and E is the electric field. The polarization P is a measure of the degree of piezoelectricity of the material. It is directly related to the piezoelectric constants.

The bending forces generated by converse piezoelectricity are extremely high, of the order of meganewtons, and usually cannot be constrained. The only reason the force is usually not noticed is because it causes a displacement of the order a few nanometers [3]. In recent years, Wang et al. [19] developed the piezoelectric constitutive theory with rotation gradient effects. Their work elucidated the size effects problems of piezoelectric solids. According to the researchers, the piezoelectric factor reduces as the grain size decreases. They solve this problem by developing a potential function.

Pyroelectricity is a derivative of piezoelectricity where the polarization is a function of the temperature. Another subset is ferroelectricity. This is the property where some dielectrics exhibit a spontaneous electric polarization that can be reversed in direction based on an external applied electric field. Ferroelectricity is generally associated with crystalline materials or semi-crystalline materials. The defining factor here is that some pyroelectric materials are ferroelectric, however not all ferroelectrics are pyroelectric [20].

The proof of the existence of ferroelectricity in PVDF or any semicrystalline polymer is the existence of a spontaneous polarization coupled with polarization reversal. This is illustrated by the hysteresis loop of the plot between polarization and electric field [21]. At high electric fields, the polarization is non linear with electric field for PVDF.

1.3 Piezoelectric Polymers

As part of the recently developed “smart” materials, piezoelectric polymers exhibit a transformation of the sensed information into the desired response. Based on these qualities, piezoelectric polymers have been increasingly used in a rapidly expanding

range of applications such as electromechanical transducers, position sensors and vibration control actuators [12].

Many synthetic polymers, including polypropylene, polystyrene and poly (methyl methacrylate), semi-crystalline polyamides and amorphous polymers such as vinyl acetate have demonstrated piezoelectric properties. However, piezoelectric effects in these materials are relatively weak and sometimes unstable [22]. Strong and stable piezoelectric properties have been observed only in the synthetic polymer polyvinylidene fluoride (PVDF or PVF₂) and PVDF copolymers [17].

For piezoelectric polymers, certain critical elements exist in terms of their ability to remain piezoelectric and these criteria are regardless of morphology. These elements, as mentioned [20], are summarized by Broadhurst and Davis [23] are: (a) the presence of permanent molecular dipoles, (b) the ability to orient or align dipoles, (c) the ability to sustain this dipole moment and (d) the ability to undergo large strains when mechanically stressed [23].

Piezoelectric polymers also have higher piezoelectric stress constants that enable them to perform better as sensors than ceramics [20]. These polymers also offer the ability to pattern electrodes on the film surface, and pole only selected regions like interdigitized electrodes.

PVDF, as with the other piezoelectric polymers, is semicrystalline. It has a polar crystalline phase which enables this phenomenon. The morphology is typically of certain crystalline regions distributed within an amorphous region [24]. The method of preparation of these polymers in a great way aids these characteristics. The final process in preparing the piezoelectric PVDF (β phase which will be discussed later) is stretching. This aligns the amorphous phases in a plane and allows the crystalline phase to rotate in

an electric field [25]. The stretching of the polymer can be both uniaxial and biaxial and this plays a role in the determination of the properties.

Owing to the composite nature of the films, free charge plays an important role in addition to dipolar polarization [7]. The requirement for it to be piezoelectric and stable, is that the free charge must be distributed throughout the film volume in such a way as to eliminate the localized electric field generated near to crystallites during dipolar reorientation.

For semicrystalline polymers, the amorphous phase supports the crystal orientation and the polarization is stable upto the Curie temperature [20]. The Curie temperature of a ferromagnetic material is the temperature above which it loses its characteristic ferromagnetic ability. For a piezoelectric it is the temperature above which the material loses its spontaneous polarization and piezoelectric characteristics.

A large amount of literature can be found on these special smart materials. Piezoelectric polymers are an important part of the encyclopedia of smart materials [26].

1.4 PVDF

PVDF has the repeated monomer unit $\text{CH}_2=\text{CF}_2$, is a gas at room temperature and pressure and is relatively stable. The solubility is less than 0.02/100g of water at room temperature. It is a semicrystalline polymer, having its glass transition temperature at $-35\text{ }^\circ\text{C}$ [6]. The toxicity of vinylidene fluoride is low but care is taken for heating and melting as it produces HF which can be dangerous [27].

Commercially it is prepared by addition polymerization or by pyrolysis reactions. Its properties can be got easily as it is a common polymer. Figure 2 shows the structure of PVDF.

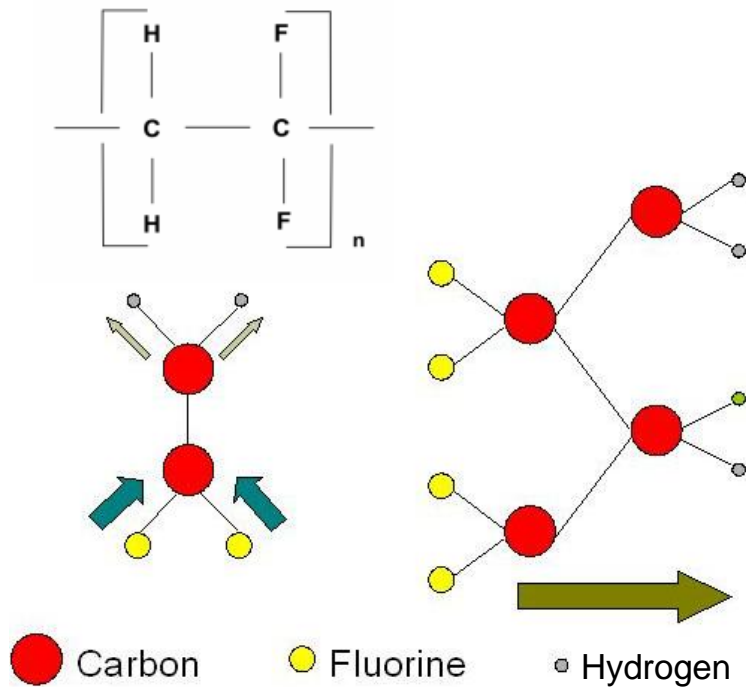


Fig. 2 Structure of PVDF

PVDF is polymorphic and can crystallize in 5 different forms. Lovinger [25] reviewed the various polymorphic structures and properties of PVDF. The major crystal forms of PVDF involve different chain conformations each of which possesses a component of a net dipole moment perpendicular to the chain.

The polymer chains of PVDF pack the unit cell in two different ways. Either they are additive and the crystal possesses a net dipole or they pack with dipoles in opposite directions so there is no net dipole in the crystal. The polar conformations are piezoelectric while the antipolar ones are not. Commercial polymerization under standard conditions usually generates alpha phase of PVDF. This is an antiparallel array and there is no net dipole in the crystal [17].

The beta phase of PVDF has a net dipole moment and the best piezoelectric coefficient after the poling process. Hence β phase is the most important in terms applications and a lot of research is being done on it. The β phase has all-trans although successive $-\text{CF}_2$ groups must be deflected by 7° in opposite directions from planar zigzag conformation to accommodate the fluorine atoms [28]. This is shown in the figure 3. The polymer chains are transformed from alpha to beta phase when the films are stretched or rolled by deformation at below 100°C , or under continuous high electrical field [17].

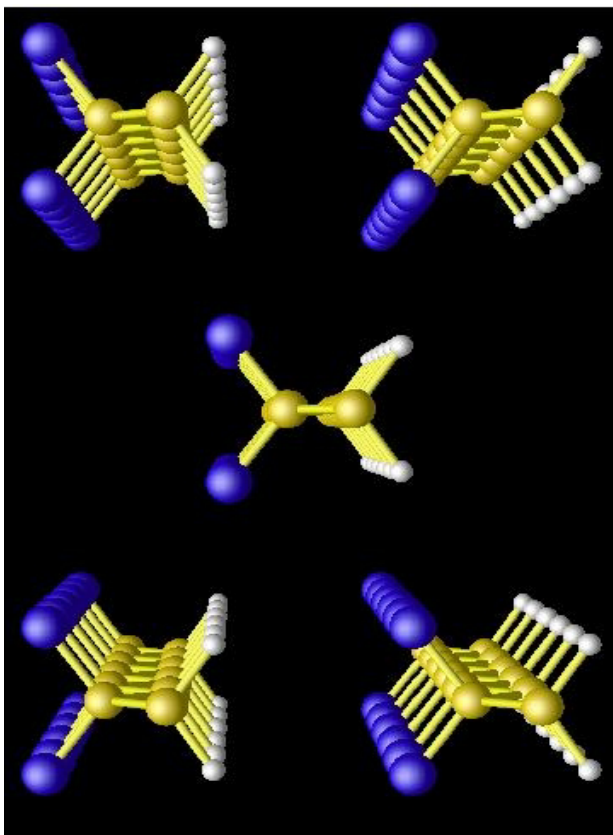


Fig. 3 β phase of PVDF [29]

The β phase has an initial random orientation of crystallites and there is a zero net polarization until the crystallites become preferentially oriented by the application of poling by an electric field.

The other polymorphic phases are gamma, delta and beta which are generally not common. These phases usually have a net dipole moment with components parallel and perpendicular to the chain axes.

The spatial symmetry disposition of the hydrogen and fluorine atoms in the chain of PVDF gives rise to unique polarity effects that influence the electrical properties. Experimental investigations have shown that deformation of textured films of PVDF after their polarization and exposure to strong electric fields induces changes on their surface. This validates the presence of piezoelectric activity in this polymer [7].

Besides the high piezoelectric coefficient, their advantages such as flexibility, biocompatibility, lightness, and low acoustic and mechanical impedance make PVDF a favorable material for bio and MEMS applications and also as transducers [3, 12]. The fact that they are not too expensive or difficult to produce aids in their use as piezoelectrics.

After the first introduction of the piezoelectric properties of PVDF by Kawai [7], novel methods to obtain the piezoelectric beta phase directly and easily have been developed [30-32].

Kobayashi et al. [33] studied in detail about the crystalline forms of PVDF. A detailed discussion about PVDF and its functionality can be found in the encyclopedia of smart materials [26]

Surface characterization of the electro active polymers has been conducted in the past [34]. Perez [35] reported in using an AFM to measure piezoelectric properties of polymers.

1.5 Actuators

An actuator is an important application of a piezoelectric. Here the principle of inverse piezoelectricity is used to get an output of deflection based on the application of an external voltage on the sample. Piezoelectric polymers are increasingly considered as favorable materials for micro-actuator applications due to their fast response, low operating voltages, and greater efficiencies of operation [36].

There have been reports to develop compact, lightweight electromechanical actuators based on electroactive polymers (EAPs) [37]. The basic building blocks of these actuators are sandwich like composite-material strips, containing EAP layers and electrode layers that bend when electric potentials are applied to the electrodes [38].

Microactuators are potentially used in MEMS devices. The advantages of using PVDF as an actuator is in the fact that it has a low Young's modulus of elasticity and this can facilitate larger strains, thereby helping the actuator achieve greater deflections and displacements [39].

Work has been done on PVDF actuators including the development of an active vibration isolation system, which incorporates piezoelectric actuators made of PVDF polymer to dampen systems in microgravity [40].

Individual sheets of PVDF do not have large displacement when voltages are applied. Hence unimorph or bimorph configurations are created. A unimorph is a cantilever that consists of one active layer and one inactive layer. In the case where active layer is piezoelectric, deformation in that layer may be induced by the application of an electric field. This deformation induces a bending displacement in the cantilever. The inactive layer may be fabricated from a non-piezoelectric material. A bimorph is a cantilever that consists of two active layers. These layers produce a displacement via electrical

activation as in a piezoelectric bimorph. The electric field causes one layer to extend and the other layer to contract.

In general, PVDF is a better sensor than it is as an actuator. However this thesis studies at the surface phenomena of PVDF and focuses on actuation characteristics for fundamental investigation.

Research efforts on PVDF or any piezoelectric polymer as an actuator have been reported before [39]. Artificial muscle actuators are most sought after applications for the electroactive polymers [41, 42]. Recently the focus has been on developing an electrode coating that is not metallic and can help the flexibility and usage of the polymer as an actuator easily [43]. Specific cases involved polymer coatings that help forming a bimorph structure easier [43, 44]. Vinogradov et al. [45] also worked on the damping and electromechanical losses in PVDF during actuation which is discussed in a later section. Paquete et al. [46] developed some low temperature characteristics of polymeric actuators that help understand the subject better. Hackl et al. [37] have developed a mathematical model for these actuators. Dargahi et al. [47] discusses about the theoretical and experimental methods in using PVDF as transducers.

1.6 Microgripper

A polymeric microgripper is a novel device that makes use of the piezoelectric properties of the polymer and incorporates it into practical usage. An essential component of all microgrippers, as of any micro-electromechanical systems (MEMS), is an actuator, which provides the required grasping motions and generates applied force to make the device operate as a gripper or tweezers [48].

Since the advent of micro scale manufacturing and advances in biological applications, there is a great need for a gripper with a tactile operation for micromanipulation. Feedback controlled manipulation is especially important for reliable and efficient

handling of micro scale objects in uncertain environments [11]. The justification for this work comes from the wide applications of microgrippers in science and industries currently. In microrobotics areas, sensorized microgrippers are essential for assembly and testing of microsystem components for high precision and reliability [10, 49, 50]. A couple of direct examples will be in surgery, where there is the need to replace tweezer-type grippers which damage the object in consideration, and in atomic force microscopy, to easily pick up the tip without damaging it.

The force-voltage characteristics of Polyvinylidene Fluoride (PVDF) can be manipulated easily so as to give a good control over the gripping. Currently there are a wide variety of Electro Active Polymers being used in these applications. However, there have been some limitations. These include low mechanical energy density and lack of robustness [42]. PVDF has potential to be a microgripper because of its good piezoelectric properties.

Previous work on PVDF microgrippers has focused on characterizing the force-voltage curves [11, 50]. Kim et al. [11] developed a PVDF based sensorized microgripper and fabricated it. Figure 4 shows the sketch of this design. Rossi et al. [51] developed a skin-like sensor based on PVDF film. We incorporate the basic idea from these designs in our system. We further characterize the frictional and adhesion forces for the surface of the microgripper.

One of the key functioning criterions of a micro gripper is its surface friction as this directly impacts its gripping force and operation. It has been reported that it is indeed friction, and not texture, that dictates grip forces during object manipulation [52]. If the friction is not optimal, then the whole purpose of the gripper is lost as the object may either slide out or be damaged due to the force applied. The motivation and contribution of this research is to study the frictional behavior of a gripper under the influence of applied electrical potential.

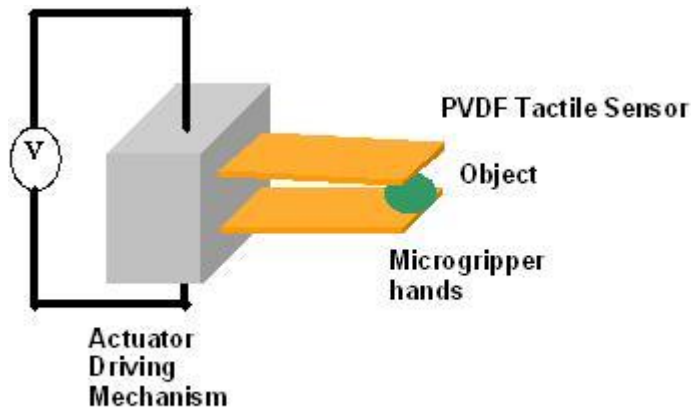


Fig. 4 Tactile microgripper, adapted from the design by Kim et al.

1.7 Motivation

There are two major objectives in this research. One is to illuminate the effect of the application of an external potential on the PVDF sample as in the case when it would be used as an actuator. The other is to develop fundamental understanding of tribological properties as well as effects of microstructures on piezoelectricity.

There is little known about the frictional behavior of piezomaterials. The uniqueness of the piezoelectricity and its effect on friction are fundamentally interesting. This can be done through experimental investigation using tribological testing. Experimentally, the tribotesting of the PVDF is followed by surface characterization and profiling. For its usage in an interesting application like the microgripper, actuation performance is also characterized. A description of the final design for this application is also discussed.

Overall this work hopes to bring forth an interesting scientific discovery and tries to use science in a practical application, thereby serving the true meaning of engineering.

The following sections are divided in the following sequence. Section 1 introduces the background of piezoelectric materials and other aspects of the project. Section 2 discusses the various theories and principles used in the research work. Section 3 presents the various experimental techniques followed in this work and their results are illustrated in Section 4. A detailed discussion of the various results obtained with a scientific perspective and a logical conclusion are highlighted in Sections 5 and 6 respectively.

2. THEORIES AND PRINCIPLES

2.1 Friction Characterization

Tribology is the science and technology of interacting surfaces in relative motion. It is a very important aspect of surface characterization as it gives a definitive idea of how a material behaves on interaction with other materials.

Friction characterization is done by tribological analysis of the sample using a tribometer. A tribometer is an instrument that measures friction on a surface by various methods, one which is a ball sliding on the reference surface and giving a relative friction value.

Our apparatus for this purpose involves a pin-on-disk tribometer, from CSM Instruments used for the measurement of the coefficient of friction (μ). Figure 5 shows the setup of the tribometer.

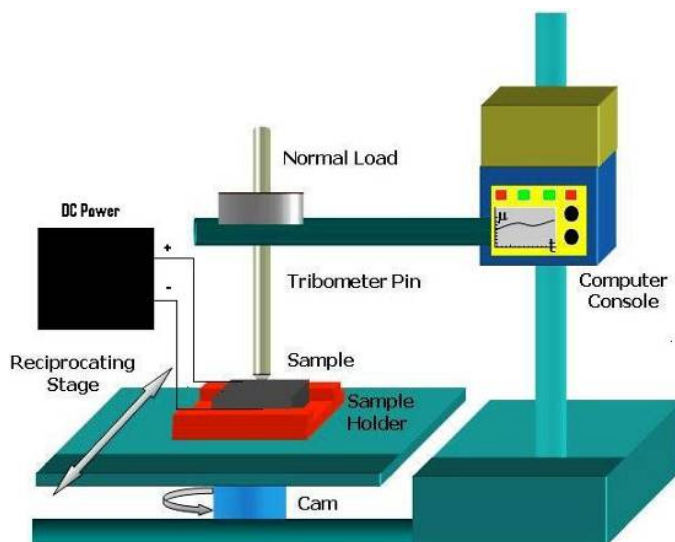


Fig. 5 Tribometer setup

The configuration is of the pin-on-disk tribometer. The pin is mounted on a stiff lever, designed as a frictionless force transducer. As the disc is sliding, resulting frictional forces acting between the pin and the sample are measured by very small deflections of the lever [53]. The strain gauges transmit these to the computer which gives the output. Figure 6 shows this configuration in detail.

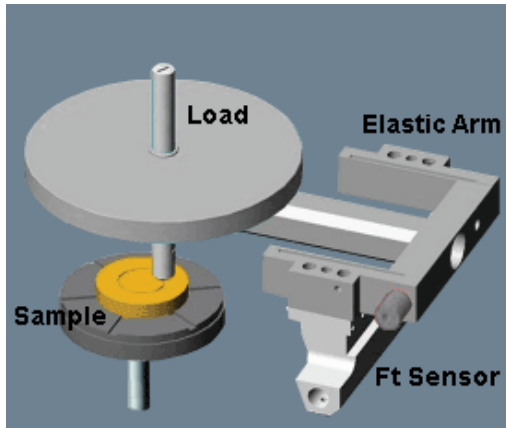


Fig. 6 Pin on disk configuration [53]

Since we know the normal load applied, and we get the tangential load from the transducers (strain gauges), we can get the coefficient of friction of the sample. This method facilitates the determination and study of friction and wear behavior of almost every solid state material combination, with varying time, contact pressure, velocity, temperature, humidity, lubricants, besides other factors [53].

We use the software TriboX for measuring and recording these data values and updating with a plot of the coefficient of friction versus time. Developed by CSM Instruments again, it gives the output from the tribometer in the computer.

The software can help us set the parameters during the testing and the output is actually a sinusoidal plot of the coefficient of friction versus time. The sinusoidal plot in reality covers the entire range of friction in the sample during one stroke of the pin and the change in friction is noted and plotted.

The linearize option in the software averages out the noise in the readings and presents a linear plot of the change in the coefficient of friction verses time. This also gives out the average value of the coefficient of friction and the standard deviation. The figure 7 shows this in detail.

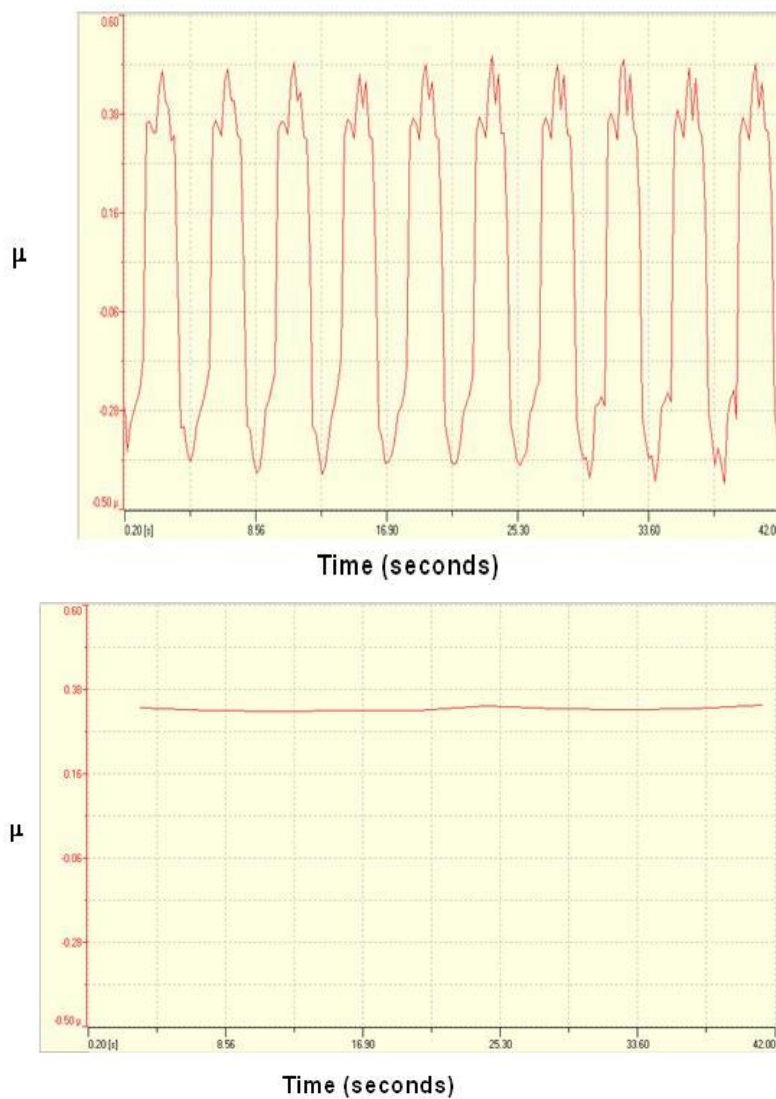


Fig. 7 Linearizing the plot of μ vs. time in the software TriboX

2.2 Surface Characterization

2.2.1 Atomic Force Microscopy

Atomic force microscopy (AFM) is a well-established surface characterization technique initially introduced for high-resolution surface profiling.

Initially, AFM studies were aimed at visualization of polymer morphology, nanostructure and molecular order, and these investigations have been performed on a large number of polymer samples [54]. More recently, the spectrum of AFM applications to polymers has broadened substantially due to the discovery of new AFM capabilities.

In addition to high resolution profiling of surface morphology and nanostructure, AFM allows determination of local materials properties and surface compositional mapping in heterogeneous samples. Furthermore, these techniques allow examination not only of the top-most surface features, but also the underlying near surface sample structure.

The following is a schematic diagram measuring surface topography using an Atomic Force microscope. The signal change from laser movement due to the cantilever movement or vibration can be detected by photo diode sensor when the probe travels the sample surface. Through the feedback loop, this signal change will be imaged by software. There are two major types of scanning modes, which are contact and close contact (or tapping mode). The contact mode AFM is useful to make clear topography image for the hard materials with low average roughness rather than soft ones. Tapping mode is useful for phase change detection and non-destructive imaging. Tapping mode eliminates the problems associated with friction, adhesion, electrostatic forces due to the surface contact on the scanning. Tapping mode imaging uses oscillating of the cantilever assembly at or near the cantilever's resonant frequency at ambient air [55]. Figure 8 shows the setup of an AFM.

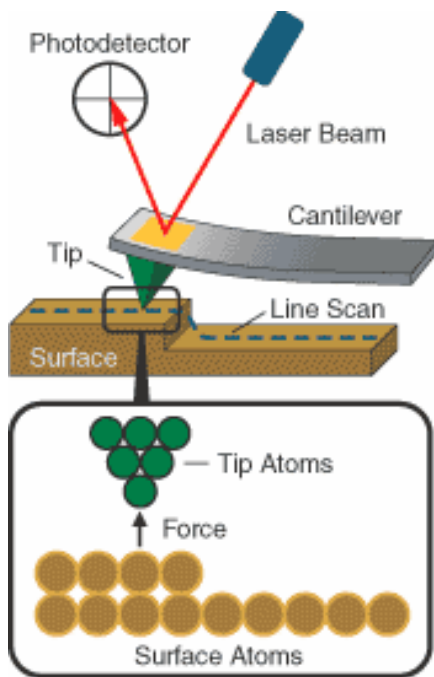


Fig. 8 Schematics of an AFM setup

Surface Characterization for the piezoelectric polymer is done by a method called the Piezoresponse force microscopy (PFM) technique is used for this purpose [56]. The capabilities of the AFM make it possible to characterize the electromechanical response of ferroelectric polycrystalline films as well as single crystals.

The basic idea of Piezoresponse Force Microscopy (PFM) is to affect locally the piezoelectric sample surface by the electric field and to analyze resulting displacements of the sample surface [57].

The PFM technique is based on the converse piezoelectric effect, which is a linear coupling between the electrical and mechanical properties of a material. Since all ferroelectrics exhibit piezoelectricity, an electric field applied to a ferroelectric sample results in changes of its dimensions. Figure 9 shows the TESE configuration for PFM.

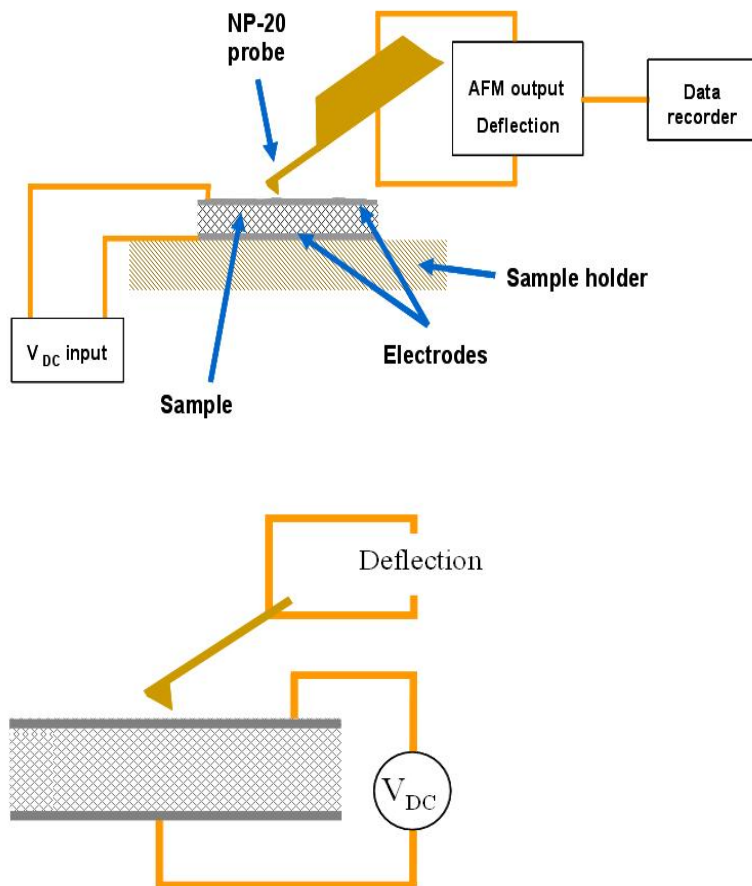


Fig. 9 AFM setup showing the TESE configuration [35]

To detect the polarization orientation the AFM tip is used as a top electrode, which is moved over the sample surface. This is part of the Tip Electrode Sample Electrode (TESE) configuration. The AFM probe tip moving according to the surface displacement causes cantilever normal or torsion (because of friction) deflections. Direction of the deflection depends on the mutual orientations of the electric field and domain polarization.

In our tests, we use the PFM method to characterize the sample respond to applied potential. The experimental part will discuss about these further in detail.

2.2.2 Surface Profilometer

A secondary means of surface characterization of the samples besides the AFM is the use of a surface profilometer. This device gives out a surface roughness value besides generating a profile view. Figure 10 shows this device in detail.



Fig. 10 Surface profilometer TR 200 and the probes used [58]

The TR 200, from Microphotonics, is a portable surface profilometer. Its display features include a detector stylus position indicator, direct display of parameters and profiles, direct printing, calibration through software.

The profilometer works on the principle of gauging the height differences across the surface of the sample, thereby giving a plot of its surface profile. The stylus rubs against the surface and its movement gives a plot of the surface profile [58]. It has a set of transducers that supply the data onto the software. This gives us not only the surface profile plot which can be used to measure relative height differences between various points, but also helps us calculate the overall surface roughness and other parameters which are useful to get a better idea of the surface in itself.

The figure 11 shows a sample profile plot obtained from the TR 200.

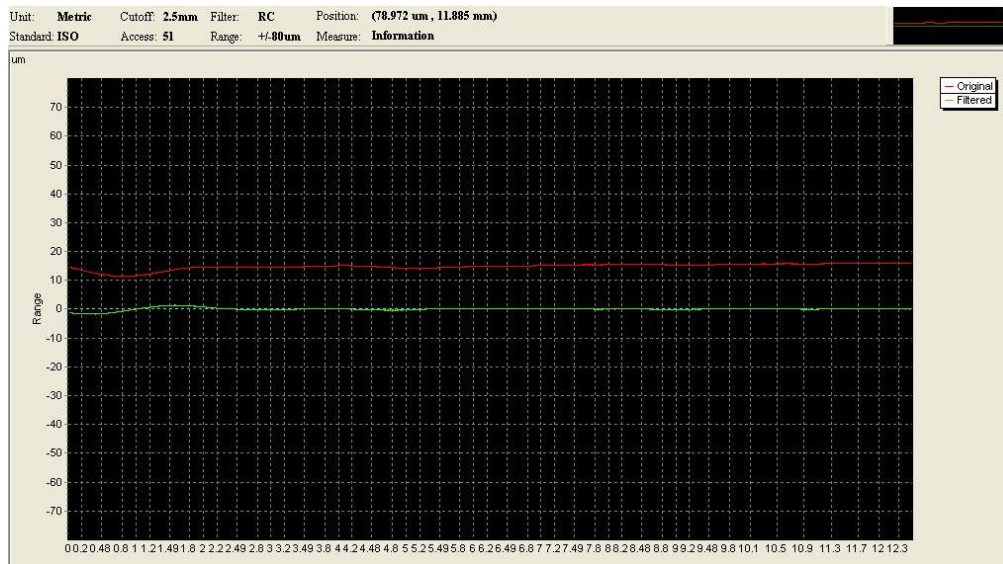


Fig. 11 Sample profile plot from the profilometer

2.3 Actuation

As discussed in section 1, individual sheets of PVDF do not have sufficient displacements when voltages are applied. Hence bimorphs and actuators are created with the material [59].

In the present research, a simple configuration of an actuator was considered. Besides designing an actuator, its performance is to be optimized for effective gripping. Thus, the gripping force (friction) and deflection under applied electrical potential are important.

The figure 12 shows the basic working of any actuator.

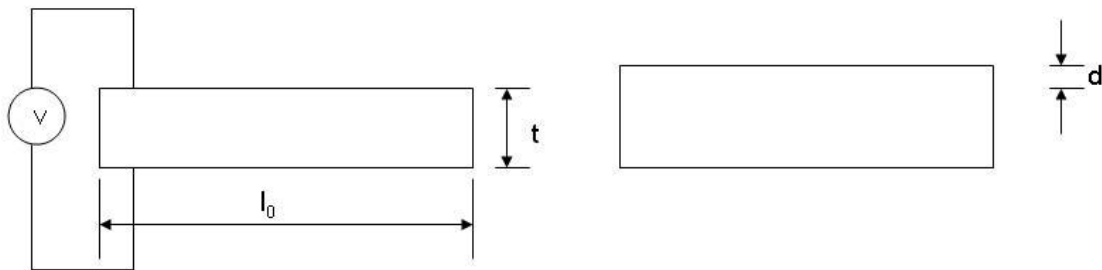


Fig. 12 Actuation of a polymer

The equation for theoretically calculating this actuation is given by

$$\Delta l / l_0 = (d_{33} * V) / t = (2 * d * t) / l_0^2$$

$$V = (2 * d * t^2) / (d_{33} * l_0^2)$$

where l_0 is the initial length, d_{33} is the piezoelectric constant, d is the thickness increase, t is the thickness of the film and V is the applied voltage. Based on these we can plot a theoretical relationship between applied voltage and dimensional changes for the sample. This relationship is derived from the constitutive equations of piezoelectricity that relate the mechanical and electrical properties.

The deflection is obtained on the sample due to the application of voltage. On the removal of voltage, the sample returns back to its neutral position or beginning position. The configurations for deflection are discussed in section 3.

This is directly related to the phenomenon of inverse piezoelectricity, which is basically the contraction or expansion of a piezoelectric crystal under the influence of an electric field. Figure 13 shows this effect.

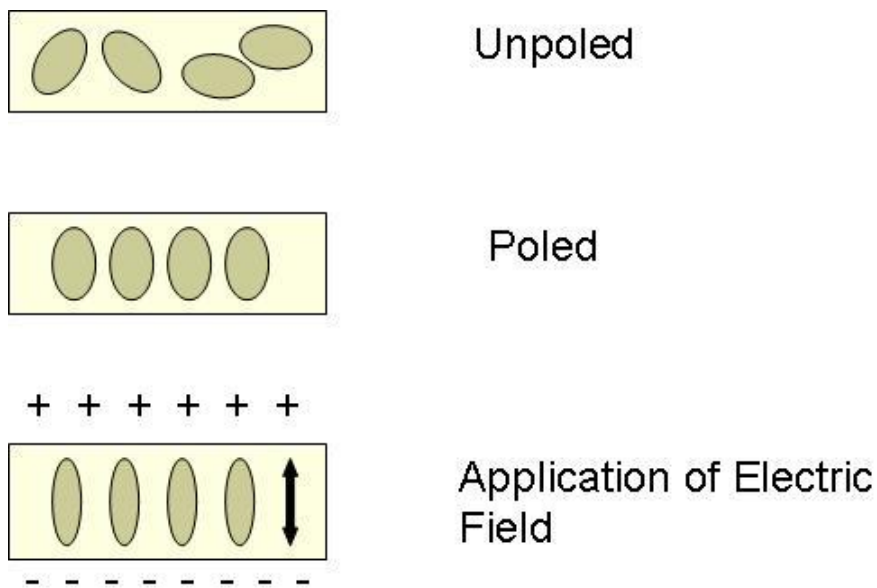


Fig. 13 Effect of application of external electric field on PVDF

One of the commonly reported problems as far as actuation of an electroded PVDF sample is the electrode itself. Gold electrode is easily corroded on the application of glue or an epoxy resin. Also the overall flexibility of the system is reduced drastically with the gold electrode as it renders the polymer stiffer and not easy to bend and contort.

Recent development has lead to the utilization of polymeric conducting electrodes, i.e., poly (3, 4-ethylenedioxythiophene) (PEDOT) [43]. This development eliminated the problems of metallic electrodes.

Another problem with actuation is that the sample may bend beyond its elastic limit. This means the spring back of the sample to its original position on the removal of voltage by elastic recovery is not possible. Also sometimes the voltage applied may be higher than that the electrodes can handle and the sample itself can be burned. Dargahi et al. [47] conducted basic analysis of the actuation of PVDF. They were able to use theoretical model to validate experimental measurements.

2.4 Microgripper Design

The basic idea involves an actuating mechanism that can be attached to the existing microassembly that allows freedom in X, Y and Z movements. The basic function of the gripper has already been discussed in detail in the introduction section. The main principle is to apply the voltage to the PVDF samples that are cut out like the fingers and actuate them so that they can deflect enough to grab the object in mind and use the microassembly to perform the X, Y and Z movements.

The microassembly setup is the one given by Velmex Inc., BiSlide System. This is shown in figure 14. The gripper has to have an attachment that will help mount the device onto this particular system.

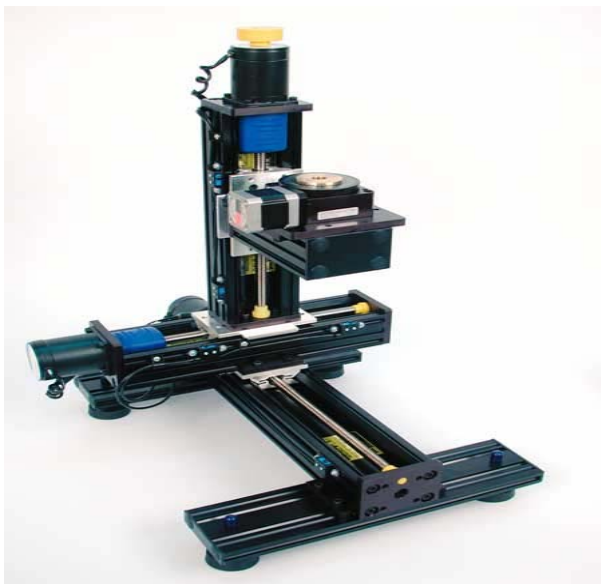


Fig. 14 BiSlide system [60]

The gripper is designed such that the dimensions of the attachment meet the required matching dimensions of the BiSlide System shown here. The basic design of the gripper is from that of Kim et al. [11]. The design for the gripper has to include the proper channels for the application of the external voltage on the polymer for actuation. The

movement of the PVDF is in 2 dimensions only and to a scope of gripping an object of a thickness of a couple of microns. The elastic modulus of the polymer sample will ensure that the polymer can lift the sample in question.

The variables that have to be kept in mind are the deflection distance, dimensions of the surface contact (both in the order of microns), the applied voltage and the force characterization.

The actual design for the microgripper is discussed in a later section. As already mentioned before this work is limited to the design and characterization of the system and the actual working model of the gripper is not worked upon due to time considerations.

3. EXPERIMENTAL

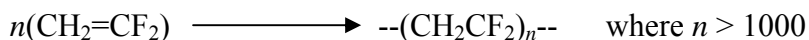
3.1 Materials

3.1.1 Synthesis of PVDF Films

PVDF films can be made from the granular PVDF purchased from ATOFINA Inc. The synthetic process of this polymer accompanies gaseous pyrolysis reactions. The preparation reactions of VDF are known by following chemical equation [61].



Polyvinylidene Fluoride polymer is prepared by the polymerization reaction that is produced by addition of monomer to monomer unit.



The first step in the process of film making is making a solution of PVDF.

PVDF solvent dimethylsulphoxide (DMSO) is used to dissolve the PVDF. The reason for using a polar solvent like DMSO or dimethylfluoride (DMF) is so that the polarity of the polymer is maintained in the solution. The acetone (80 ml) and DMSO (20 ml) solution were added to all the PVDF. The amount of PVDF is based on the desired viscosity. Usually around 35% of PVDF by weight will ensure a good solution that is easily pourable. A hotplate with stir was used at a temperature of 40°C to dissolve the PVDF in the solution rapidly. It takes 30min to 40min to dissolve PVDF completely.

The beaker containing the solution is immediately wrapped with paraffin tape. This will ensure that the acetone that has evaporated will cool down and condense within the solution in order to maintain a constant concentration.

The next step in the process of making PVDF films is to perform the solution casting. This operation in our case is performed using a doctor blade system. The solution of PVDF is poured in between the plates and the blade is drawn across the surface to ensure it being locked in. The entire setup is put in the oven and left overnight for a temperature of 400 °C. This solution casting process gives us the PVDF films in the alpha phase, which is normally obtained while cooling from the melt. Figure 15 depicts the solution casting process.

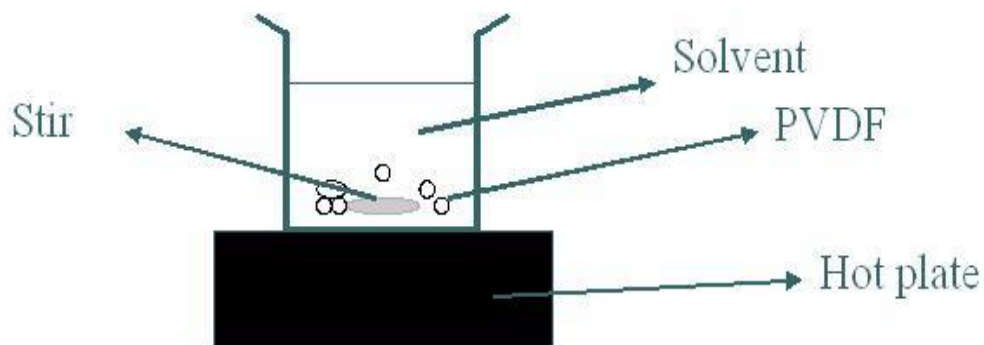


Fig. 15 Solution casting of PVDF

As we have already discussed, there is a strong dependence of the piezoelectric and pyroelectric activity upon the film orientation, crystalline structures, and the state of polarization. The beta phase is the most important of the PVDF polymorphs and is the one used extensively in various applications. It can be obtained by mechanical stretching of the alpha phase PVDF at temperatures below 130 °C.

The next step in the procedure of making the beta phase films is the mechanical extension. Semicrystalline polymers always have to be stretched between their glass transition temperature T_g and their melting point T_m [17]. The stretching temperature, extension rate and degree of extension play an important role in this process and determine the final properties of the film. The principal change that occurs during this stretching is the preferential alignment of the molecular chains in the direction of

stretching in the amorphous and crystalline phases. This makes the non polar alpha phase into the polar beta phase.

Uniaxial stretching in an Instron tensile testing apparatus is the preferred method. This is done to an extension of 350% of the original length. Stretching is usually done at 80 °C to get optimum results [25].

The stretched film will be in the beta phase. However as discussed before, the dipoles in the polymer will still be unoriented. Unoriented PVDF films do not have piezoelectric activity. Hence an external poling is done to ensure the activity in the polymer. There are different methods to do this poling, however the most preferred one is corona poling.

Application of a corona discharge at high potential in the vicinity of the film, with the opposite side grounded leads to orientation of the dipoles in the polymer. This process can be completed in a few seconds itself at room temperature [62]. Corona poling can also be done at elevated temperatures [17]. The system basically consists of the sample in contact with a metal electrode. The charge is supplied by a needle electrode at a short distance. Corona is self persistent electrical discharge in a gas where the laplacian electric field limits the primary ionization process to regions near to high field electrodes [63]. The figure 16 describes the whole process of making beta phase PVDF films in detail.

Another novel method to produce poled PVDF films in beta phase was discussed by Taekwon Jee [64] in his work on In Situ Poling of Spin cast films. The phase morphology of these films after these processes is verified by various methods like Fourier Transform InfraRed Spectroscopy (FTIR) and Wide Angle X-Ray Diffraction (WAXD) to ensure the beta phase.

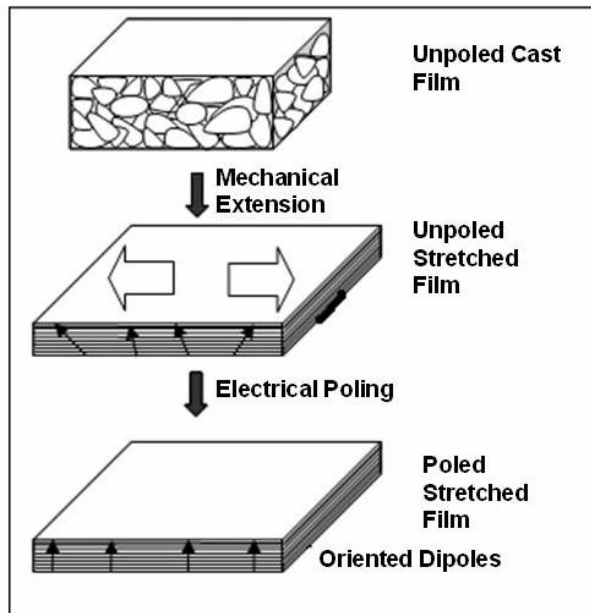


Fig. 16 Procedure to make PVDF films

Besides using polling experiments to make samples, commercial PVDF were also used. The PVDF sheets were purchased from the Measurement Specialties Inc. Table 1 lists the types of samples we tested. Both poled and unpoled PVDF were used in all the tests including assessing the effect of piezoelectricity on the coefficient of friction. The basic difference between the poled and the unpoled samples is that even though they are both in the beta phase, the unpoled sample is not piezoelectrically active. The process of making both the unpoled and poled films is described in figure 16.

The PVDF samples are cut into a size of 35 mm by 10 mm. This is a standard size made for all the experiments to follow. The basic reason for this is to get a sample size big enough to be able to test in the tribometer and other characterization possible on its surface.

3.1.2 Electroding

In order for the PVDF to be used as a piezoelectric in our tests or for any application, there must be a way to pass an electric field onto it or get an output voltage from it. This is not possible directly on the sample as PVDF by itself is an insulator. For this purpose, surface electroding was performed using sputtering technique. Usually the gold electrode is preferred because of its good conductivity.

When a target is bombarded with fast heavy particles, erosion of the target material occurs, i.e., sputtering. The arrangements of the systems are such that some of the sputtered atoms will condense on the surface of the specimen to be coated. This is done in a gaseous environment that enhances the coating of the target material on the sample [65].



Fig. 17 Hummer sputtering system

The figure 17 shows the hummer sputtering system by Anatech Corp. The target is made suitable for a gold electroding and the gas used is argon. Some important specifications of the system include anode and dark space shield attract heat bearing electrons away from the sample, grain size less than 2 nanometers and Automatic vent at process termination [65].

The samples are electroded for a thickness of around 100 nm gold, in the Hummer Sputtering System, run at 15 mA and 70 mTorr for 20 minutes. This is done on both sides so that the wires can be attached to the surfaces directly and application of voltage on the sample is easy.

3.1.3 Sample Materials

Of the samples that were used, the poled, stretched PVDF was 52 μm thick while the unpoled, stretched PVDF was 110 μm thick as shown in Table 1. Sample A was the poled and stretched PVDF with a thickness of 52 μm . Sample B was the poled and stretched PVDF of 52 μm thick. However, it was tested by measuring the friction perpendicular to the direction of stretching. For sample A, the friction direction was along the stretching orientation. The sample C was unpoled but stretched with a thickness of 110 μm .

Table 1 Description of the samples used

Sample	Poling Nature	Thickness(μm)
A	Poled	52
B	Poled	52
C	Unpoled	110

The only factor to be considered while using these commercial films is that the original polarity of the samples is not known. The way we counteract this is by performing a test with a reverse polarity such that the sample is tested for both signs of the applied voltage. The characteristics of the sample become clearer if they are tested in this situation and the role played by the polarity of the sample is displayed. This will be discussed further in the following sections.

The figure 18 shows a sample after being electroded ready for testing.

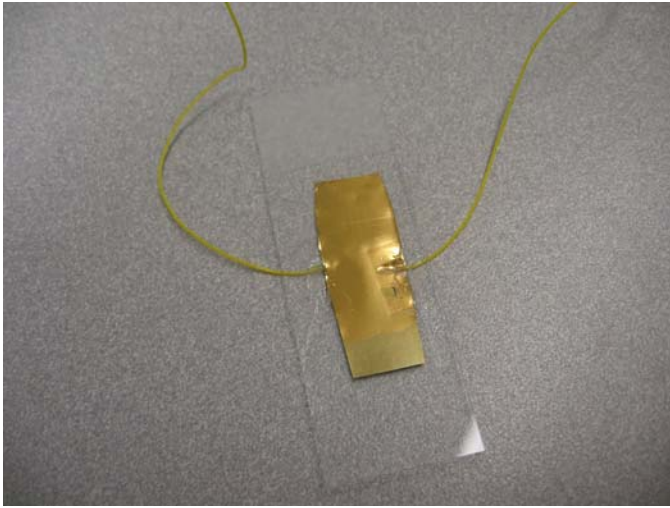


Fig. 18 Sample for testing

After this, the tribological characterization is done on all the samples.

3.2 Friction Testing

A CSM pin-on-disk tribometer was used for friction study. Details of the tribometer were discussed in section 2. The pin was replaced by a small piece of PVDF that was glued on to the pin. This PVDF slides against another disk of the same material.

In our tests we analyze the PVDF – PVDF contact friction. The reason for using this setup instead of a ball on disk type testing is because we do not want to damage the surface of our sample. Also the PVDF is an insulator and prevents building up charge on the metal pin on application of voltage.

In this study, all the test parameters were fixed to the same conditions. The reciprocating speed was set at 0.15 cm/sec. The distance of one stroke was 5mm as the half amplitude of one complete cycle. The normal force applied was also constant at 1N. All the tests were done for a duration of 10 cycles in reciprocal motion. In addition, experiments

were carried out at room temperature with the relative humidity around 75%. The contact pressure was around 15 PSI.

The voltage was applied on the sample from a DC power source. The electroded sample was fitted with wires on top and bottom such that positive charge was on the top electrode and the negative on the bottom. The sample was stuck onto a glass slide with glue. The voltage is adjusted so that the electric field remains constant for all the samples as they are of different thickness. The figure 19 shows the entire setup and figure 20 depicts the interface considered.

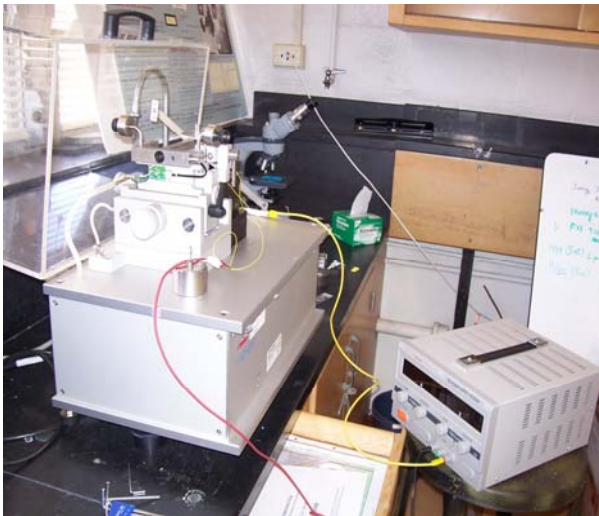


Fig. 19 Experimental setup for tribotesting

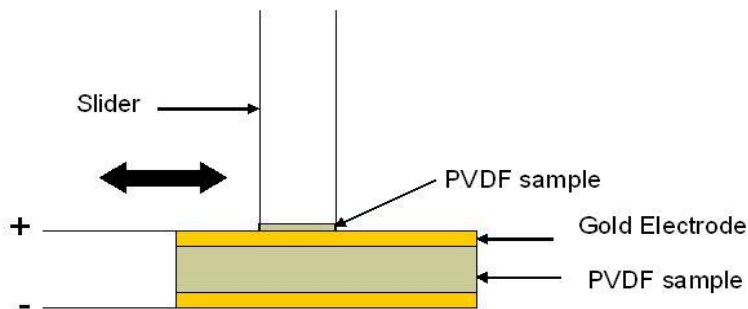


Fig. 20 Interface for tribotesting

Before performing these tests, the resistance value for each sample electrode is checked to ensure proper electrical conductivity. This was done using a standard multimeter and the resistance between the surface and the wire ends were recorded. These values were found to be approximately constant throughout the testing duration.

The setup and method of testing were assessed by characterizing applied normal force against the coefficient of friction and speed of table motion against the coefficient of friction. Both these were found to match the proper trends and confirm the validity of the setup as will be shown in the Section 4. During testing, friction coefficient was recorded. Electrical potential was applied in different directions.

The samples are then analyzed to characterize the effects of voltage on the friction. For each sample, the coefficient of friction vs. time is plotted under different test conditions. Uncoated sample was tested as a reference. The electroded sample was tested with the voltage varying from 0 to 10 V. This procedure is identical for each sample to ensure consistency in the measurements. Since sample C has a thickness that is twice of that of samples A and B, and since the electric field is inversely proportional to thickness we applied a voltage up to 20 V in the case of the unpoled sample to ensure application of the same electric field.

As described before, since the original polarity of the sample is not known, the reverse polarity tests are performed to check the effect of the polarity of the sample in this regard. Also for the poled samples, the original dipole orientation of the sample, i.e., the polarity of the applied poling is unknown. Hence this is countered by running a test by turning the sample upside down and keeping a reference side and conducting this test. The sample for this particular test is the sample A only as it really matters only for the piezoelectric sample. This test is mainly done to verify the earlier tests and get a basis to draw logical conclusions from.

Before each experiment, sample surfaces were cleaned using isopropyl alcohol. To assess the effects of reverse polarity, tests were conducted by applying negative potentials on the sample surface. The negative potential was 8V. Each sample was tested 5 times for repeatability.

The software TriboX records the output in terms of friction force during tribotesting against time. For each reciprocal motion, an average friction was obtained. The standard deviation was obtained based on the repeated experiments. Figure 21 shows the interface of the software.

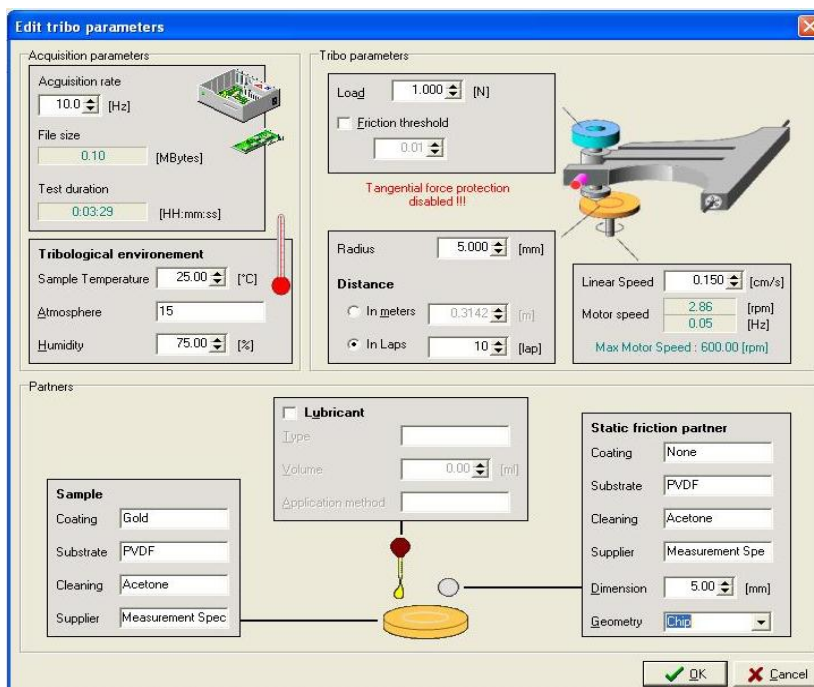


Fig. 21 TriboX software interface

3.3 Surface Characterization

3.3.1 Surface Profilometry

Surface characterization was conducted on the material includes surface roughness measurement and profiling with a TR-200 surface profilometer (Microphotonics). The

setup of the sample and the profiling are exactly the same as in the friction test. The probe slides over the surface and characterizes the surface roughness and profile. This is done with varying the applied potential on the sample.

The voltage is applied to the sample with the same method by attaching the wires to the surface and getting the input from the power source. Reverse polarity tests are also performed for the same to ensure the uniformity in the tests and check for the role played by the dipole orientation on the surface.

This test is done on all the three samples A, B and C as mentioned before. This is to identify the role played by the piezoelectric nature of the sample in this particular phenomenon. Also the reverse polarity tests are performed in the same manner described in this section.

The output from the TR200 is the plot of the surface profile and it shows any change in the sample datum levels due to the application of voltage. The surface roughness is also read out as an output that provides information of surface and change due to application of the external source.

3.3.2 AFM Characterization

Detailed surface characterization using an AFM (PNI) is performed in order to gain a detailed understanding of the surface. The Piezoresponse force microscopy (PFM) technique is used for this purpose. The capabilities of the AFM make it possible to characterize the electromechanical response of ferroelectric polycrystalline films as well as single crystals.

The setup comprises a digital instrument multimode scanning probe microscope with a Nanoscope III controller and a non-conductive Veeco digital instrument triangular NP-20 silicon nitride probe in contact mode. The probe scanning rate is kept at 1 Hz. The

spring constant of the probe is $k = 58 \text{ N/m}$ and the observed sensitivity is in the range of 40 to 60 nm/V. Figure 9 shows the schematic of the AFM. This is the setup used by the authors [35] in their work.

The sample configuration and the input and output voltage locations are shown in figure 9. As illustrated, a Tip Electrode Sample Electrode (TESE) configuration is used, where the sample is electroded on both surfaces and fixed to the sample holder by conductive glue. The input voltage is applied as shown in figure 9; it is increased from 0V to a maximum voltage then decreased back to 0V to simulate a triangular wave of frequency less than or equal to 1 Hz [35].

Contact mode scanning was conducted with multiple points on the sample surface, one at a time. Each point is subjected to a voltage varying and the tip deflection is the measured output. Once the system is calibrated using a set point, the deflection is converted to actual displacement of the sample.

The AFM images are discussed in the following sections and help us to clearly understand the surface properties.

3.4 Actuation

The actuation tests are performed in order to assess to the usage of PVDF as an actuator. This application was discussed in section 1. The two configurations tested here are the Unimorph and the basic Bimorph. The figure 22 shows this in detail.

The unimorph consists of a layer of active PVDF, electroded and attached with wires. A non active PVDF layer is stack on top of this over the wires. The bimorph has 2 active layers of PVDF stacked such that their polarities are opposite to each other and the outer surfaces are electroded and attached with wires.

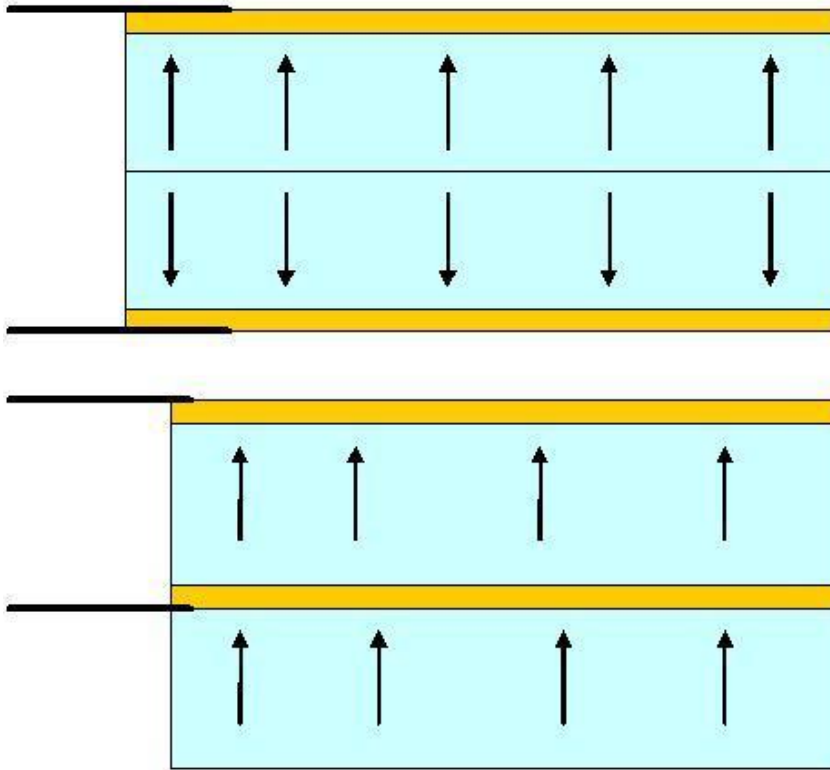


Fig. 22 Actuator configurations

The setup to perform the actuation experiments is simple. It consists of a sample holding clip that fixes one end of the sample on it. This end also incidentally houses the connections for the application of voltage. The setup is placed under an optical microscope. The initial position of the sample before the application of the voltage is set as the reference or datum. The voltage is then applied as before and the deflection of the sample is noted. The tip displacement distance can be easily measured from the datum position marked and the optical microscope gives out this measurement.

The displacement distances are plotted for each sample against the applied voltage. The plots include the theoretical displacement versus applied voltage graph also which is calculated from the equations discussed in section 2. These equations are basically derived from the piezoelectric equations of the sample which correlate the electric and mechanical constitutive equations [4].

The most important concern that should be ensured is that the voltage applied on these samples should be gradual and not sharp increments. This is because sometimes the surge of applied potential into the sample will make it deform beyond its elastic limit. This means that the sample will not return to its original position even after the removal of the applied voltage. In addition, excess of the potential may cause a short circuit in the electrodes that will burn the sample itself.

The plots give a good comparison of the actuation characteristics of the different configurations of the sample and help us in using the polymer in the microgripper application as an actuator.

3.5 Design of the Microgripper

The basic design for a microgripper made of this PVDF sample is done in SOLIDWORKS (SP4.1) from SolidWorks Inc. The design is basically one of an attachment which will fit in the microassembly discussed in section 1. The basic working of this attachment is that it provides the housing for the polymer sample to be actuated.

The design also considers the need to apply an external electric field on the sample and hence provides the channels to attach the wires on the samples. The configuration and sizes are decided based upon the results of the previous experiments.

The main point is to match the dimensions of the microassembly and remain within the scope of the project. The design of the gripper is complete and can be directly used to manufacture a prototype.

4. RESULTS

This section presents experimental results related to the PVDF samples. The content includes tribological testing and material characterization of the PVDF. A detailed design of the microgripper application is also described here. Effects of externally applied electric field were studied. The following section discusses results and mechanisms.

4.1 Friction Characterization

As discussed earlier, to serve the purpose of a microgripper, one of the most important properties is the frictional behavior. In addition, the effects of an applied external electric field on friction are as important. The scenario considered is similar to an actuator. In such, the surface friction is tested using the setup as described in section 3.

A series of tests were carried out in the tribometer and the coefficient of friction versus time was plotted. The software used for this purpose is TriboX. The graphs are initially a sinusoidal function and the friction is obtained for reciprocal strokes of the pin-on-disk tribometer. The coefficient of friction was obtained by linearizing the sinusoidal output. This process has already been described in section 2. The sinusoidal wave covers the entire range of friction on the sample during time of reciprocating rubbing contact. This motion continues through out the test and hence we obtained the average value of the coefficient of friction.

The friction coefficient as a function of speed and normal force were shown. As shown in figures 23 and 24, the coefficient of friction is a linear relationship with the relative surface speed and normal force. This is in correlation to published results. The error bars show the entire range of values of the coefficient of friction for the samples.

These plots show us that the setup and the method of tribological testing are in correlation with established results. They also help us calibrate the system to ensure uniformity in the analysis. The Amonton's laws on friction [66] are primarily verified here to ensure the consistency of the experiment and to ensure a standard with respect to analyze the samples.

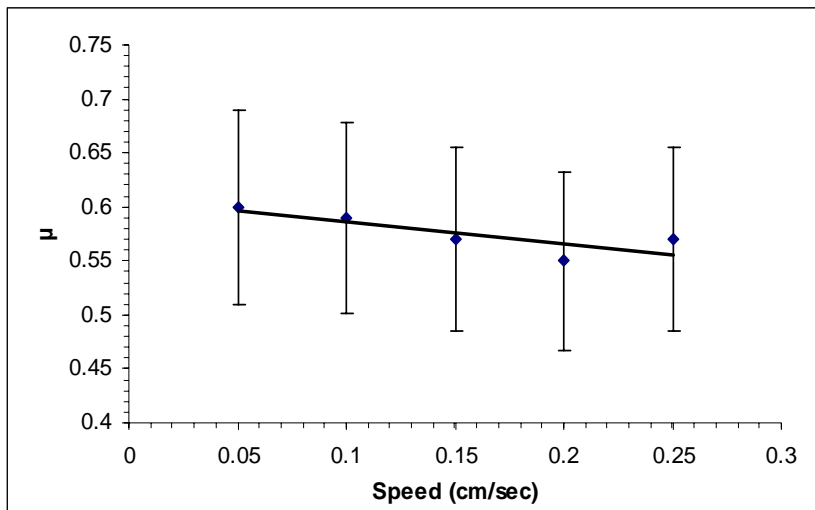


Fig. 23 Plot of speed of reciprocation against coefficient of friction

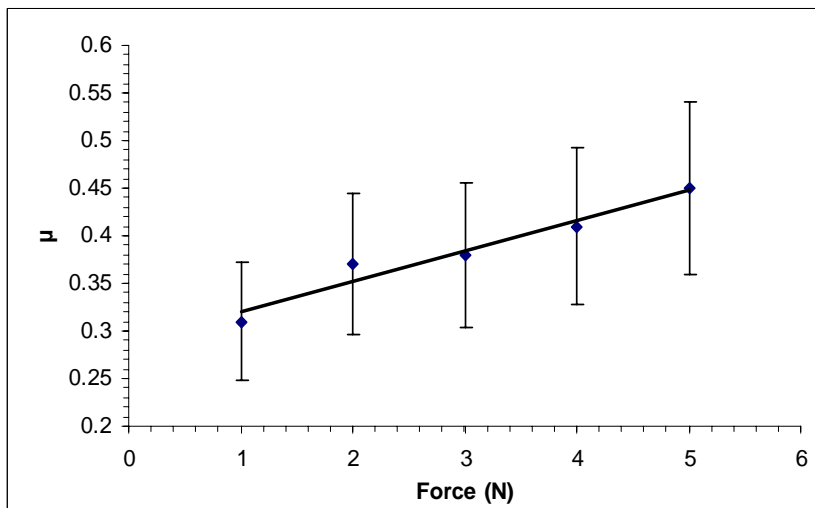


Fig. 24 Plot of applied normal force against coefficient of friction

Sample A was firstly tested on the tribometer. The friction coefficient was measured on the uncoated and coated samples respectively. The difference in these was found to be negligible in the terms of the actual increase in value, indicating that the presence of the gold electrode does not affect the coefficient of friction results. Also since all the samples are of the same electrode, the property differences will be due to the inherent differences in the sample itself rather than the electrode coating.

Next, we apply a voltage from 0 to 10V and assess its effect on the coefficient of friction of sample A. We find that the coefficient of friction value increases with the application of voltage for sample A. A factor of 1.63 is found in the increase of the coefficient of friction value due to the application of voltage in the sample, see figure 25. This increase in the friction value is repeatable to a large extent and shows an “On-Off” relationship with the applied voltage in that the overall behavior is one with an increase on the application of external voltage but also does not periodically increase with the application of this external voltage. Also the value falls back to the original value of the coefficient of friction before applying voltage when it is reverted back to 0 V.

Next we analyze Sample B, where B is also poled PVDF, but tested perpendicular to the stretching (Table 1). The other test conditions are the same. When no voltage is applied, the coefficient of friction for sample B is slightly higher than that for sample A. This can be explained by the fact that the mechanical stretching creates features on the film surface such as grooves, yielding a rougher surface and a higher friction perpendicular to the grooves. The figure 25 shows the plot of coefficient of friction vs. electric field as a comparison between Samples A and B. As shown in the figure, two curves are close to each other. The frictional behavior of two samples was found to be negligible in the terms of the actual increase in value. When the voltage is applied, analysis of the data for both samples shows a trend of friction coefficient increasing with increase in the voltage. A rough estimate shows a factor of 1.37 increase in the μ value in Sample B due to the

addition of voltage, see figure 25. Sample B also shows the same “On-Off” effect that relates the coefficient of friction to the applied voltage.

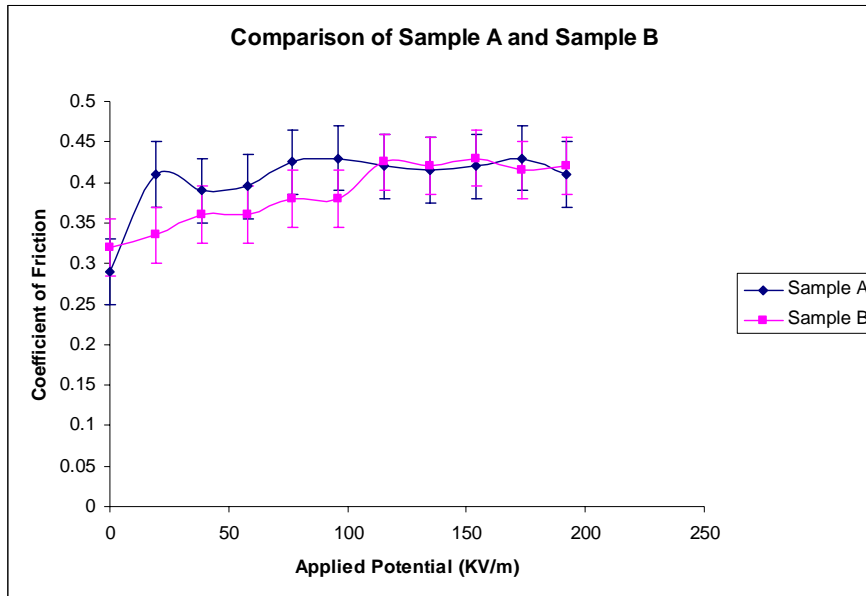


Fig. 25 Comparison of sample A and B based on μ vs. voltage

The same tests are then repeated for sample C, the stretched but unpoled PVDF.

Interestingly, analysis of the data for this sample shows a trend of friction that is not affected by applied voltage, see figure 26.

Sample C which is not piezoelectric does not show any signs of reciprocating this phenomenon observed with the piezoelectric PVDF samples.

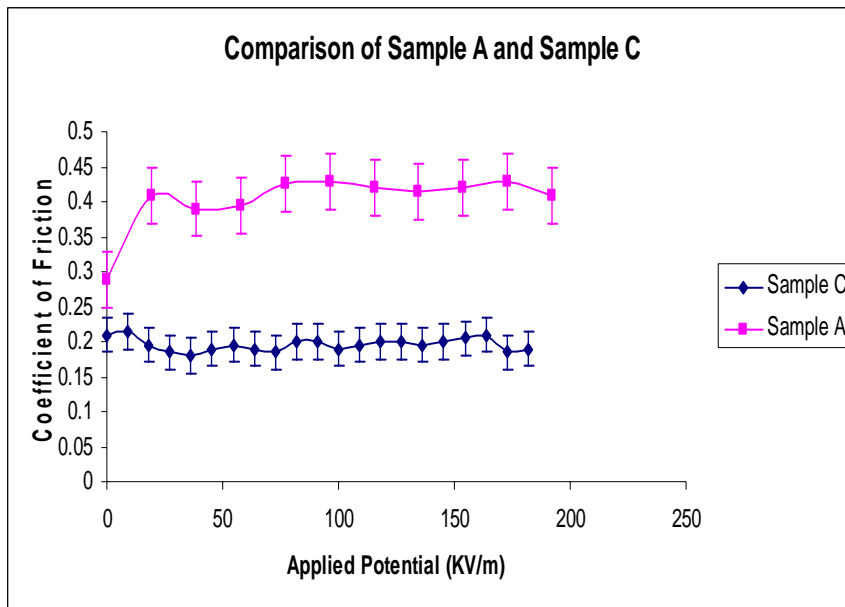


Fig. 26 Comparison of sample A and C based on μ vs. voltage

Having assessed that the voltage affects the coefficient of friction, we then investigate the role of the polarity. We perform the experiment of both reversing the polarity (by simply flipping the sample) and inverting applied voltage (by simply reversing the leads). The table 2 shows the results.

Table 2 Inverting Voltage Tests for Samples A, B and C

Sample	Voltage	μ for +ve Charge on Top	μ for -ve Charge on Top
A	8	0.458	0.361
B	8	0.448	0.396
C	8	0.221	0.218

This provides valuable information that for poled PVDF, the inversion of the leads and inverting the polarity both makes a difference in the friction values. As mentioned before, since we do not know the original polarity of the samples, we take one side as reference for two more samples. These samples are quintessentially the same as Sample

A, both being poled, stretched and electroded and having a thickness of 52 μm . We then test for the coefficient of friction at 8 V applied and then reverse the sign of the voltage. This way we can study the effect of the polarization on the friction.

Analyzing the effects of polarization and inverting voltage we see that the coefficient of friction value decreases for Sample 1 while it increases for Sample 2 on inverting the voltage leads from positive to negative, in that order. Table 3 shows these results.

Table 3 Reverse Polarity Tests

Sample	Voltage	μ for +ve Charge on Top	μ for -ve Charge on Top
Sample 1 reference side up	8	0.408	0.352
Sample 2 reference side down	8	0.453	0.523

4.2 Surface Characterization

4.2.1 Surface Profiling

After testing, we assess the surface analysis results from surface profiling characterization to better understand the piezoelectric property.

The surface profilometry results show no change in the average surface roughness (Ra) value of the samples with application of the voltage. The surface profile in addition does not have a significant variation. The figure 27 shows the plot of the surface roughness versus the applied voltage for the various samples. Table 4 details the effect on the various samples.

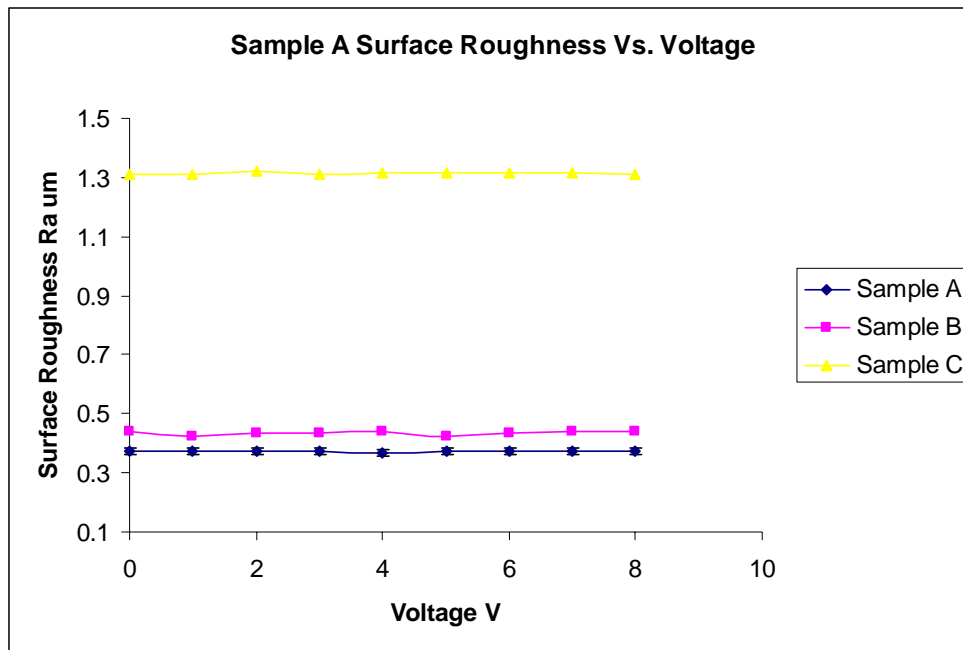


Fig. 27 Surface Roughness versus voltage for the various samples

Table 4 Surface Roughness of the samples at different voltages

Sample	R _a (μm) at 0V	R _a (μm) at 8V
A	0.373	0.375
B	0.491	0.482
C	1.313	1.312

The principles behind this from these results lie on the surface profile of the PVDF sample does not vary too much with the application of the external voltage. Even though this test is done with the exact same method as the friction testing, there is no significant variation that is expected as the dimensional changes on the surface for the given conditions of external voltage lie in the order of nanometers. Also the actual value of the surface roughness itself is at the same level for each sample with or without the application of voltage and also with the inversion of the polarity. A factor to consider here is that the surface profilometer reads out the profile variations in micrometers while the actual dimensional changes in the sample are in the order of nanometers.

4.2.2 AFM Characterization

The AFM analysis was carried out on the sample tested. Figure 28 shows the imaging results, where left shows the probe displacement versus time and the right image is the pixel. Two arrows are corresponding to each other.

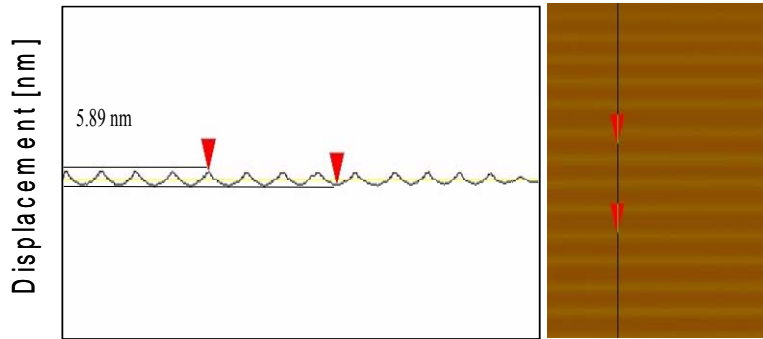


Fig. 28 AFM probe displacement with applied voltage (courtesy of R Perez) [35]

The thickness increase due to the application of voltage is clearly defined in this AFM picture. A standard silicon nitride probe is in contact with the PVDF surface without movement. A voltage is then applied at 1 Hz. In figure 28, the y-axis is the displacement of the probe and x-axis is arbitrary time. The figure shows that the displacement of the probe (associated with the thickness of the PVDF) changes along with the voltage. The total thickness change is about 6 nm. The imaging is done from point to point and the overall effect of the applied potential on the surface is obtained. The thickness increase is due to the piezoelectric nature of the sample.

Another AFM image shown in figure 29 depicts the surface of the sample better. This picture illustrates the samples microstructure. The AFM (Nano®, Pacific Nanotechnology) was operated under the contact mode with a conductive tip. External potential was applied on the sample in the same method as before. The surface was scanned and mapped before and after a voltage was applied

Of the four images shown, the two height images are shown on the left and two phase images are on the right. The height images represent the surface topography. The phase images indicate varying phases of the material. Material grains are around 5 μm in size. In the same figure, the two top figures were made with no electrical potential applied. The bottom two were obtained when a 5 Volt potential was applied across the thickness of the material.

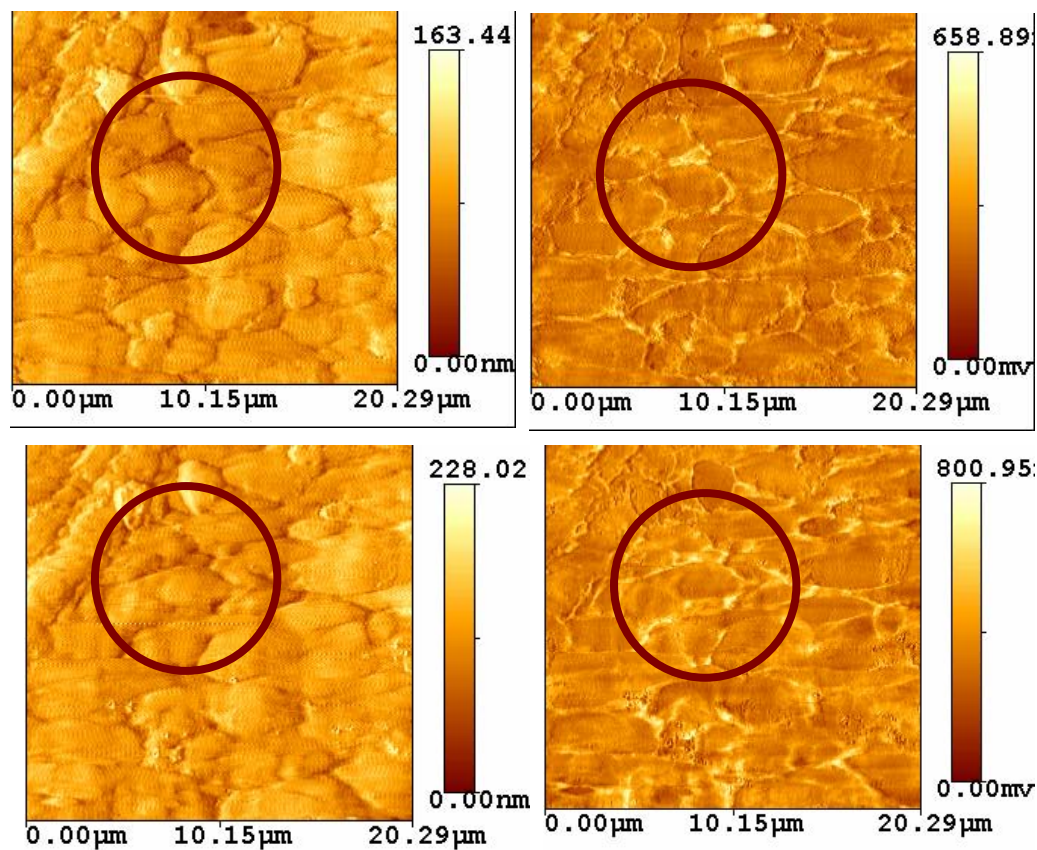


Fig. 29 AFM Images with the application of 5V (Courtesy H Lee)

The figure 29 shows the effect of the applied potential on the material in terms of its microstructure. The figure shows that in the presence of an electrical potential, the space between grains become smaller. As highlighted by the circles in the bottom figure, areas of uneven surface height seem to be “squeezed” due to the applied potential. This is thus seen on the surface. The application of the field stretches the dipoles which are already aligned.

This confirms previous tests that the piezoelectric nature of the sample leads to some surface phenomenon. The dimensional change in the sample is clearly defined in the figure 28. The test is done for the piezoelectric sample A and gives us an idea of how the properties are affected due to the external field. This serves us with not only a clear picture of the dimensional change, but also with a logical way of concluding the phenomenon of the change in the coefficient of friction for the sample. This will be discussed in detail in the next section.

4.3 Actuation

Actuation of the PVDF samples are done in the setup described before. The initial position is noted by the optical microscope and the position is marked as the datum level.

After this the voltage is applied on the samples and the deflection of the sample is observed under the microscope. The application of voltage is usually done slowly as described before. The sample is constantly observed under the optical microscope and any deflection is magnified and easily recorded using this distance bar. Based on this we find the best deflection possible for our application as a microgripper, such that for the voltage applied, the deflection is appropriate and in the range of a few microns.

Based on the equations, the plots for the standard sample theoretical versus experimental for PVDF is shown below.

Overall the plots signify a good control over the deflection of the PVDF sample in the given range as specified by the requirements for a microgripper. Figure 30 shows the deflection plots as a function of the applied voltage for the configurations.

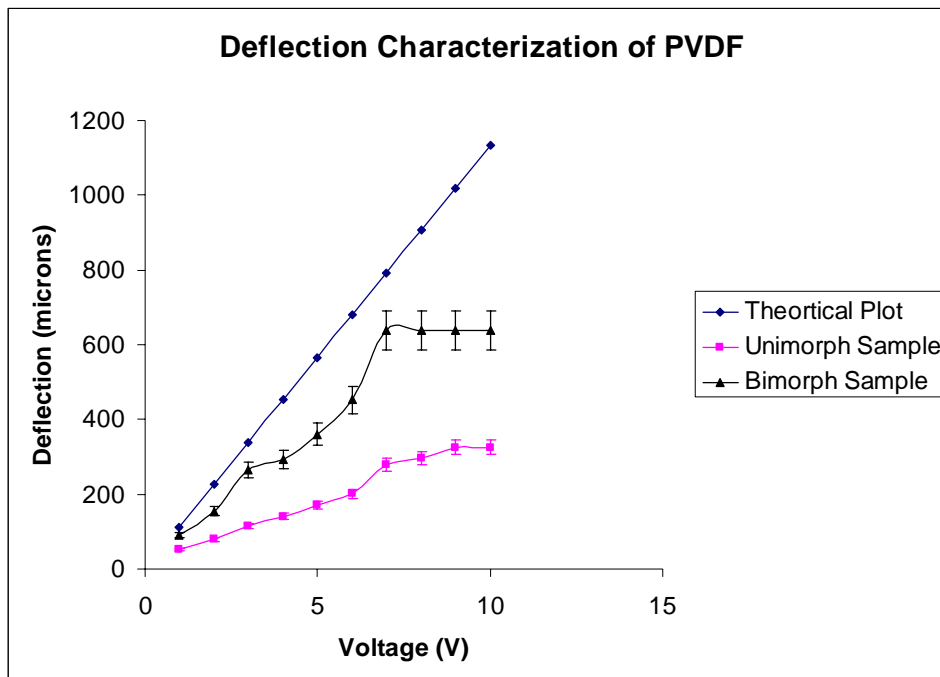


Fig. 30 Deflection characterization of PVDF

We find from the plots that the best possible configuration is the bimorph configurations with the two samples of opposite polarity stuck together. Initially for the samples it takes more voltage than the theoretical model to start the deflection as they have to cross the barrier and get enough potential flowing so as to move the dipoles and create this deflection mechanism.

Also the problem with some samples was that they deflected beyond their elastic limit and the removal of voltage did not have any effect on them. Another problem was with the gold electrode was that it rendered the sample stiffer than its original value and hence the deflection was not uniform.

4.4 Microgripper Design

The design for the PVDF Microgripper was done in SOLIDWORKS (SP4.1) as discussed before. The design considerations included to ensure the dimensional accuracy as far as mating with the microassembly setup was concerned.

The design was based to include the possibility of attaching the polymer fingers and providing channels for the wires that enable the actuation. Ease of manufacture is the key motive behind designing this microgripper. The design is based on the model developed by Kim et al. [11]

The figure 31 shows the design in detail.

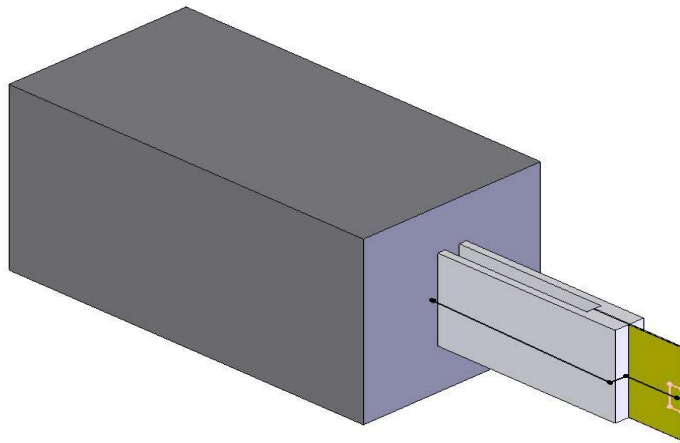


Fig. 31 Design of the microgripper attachment

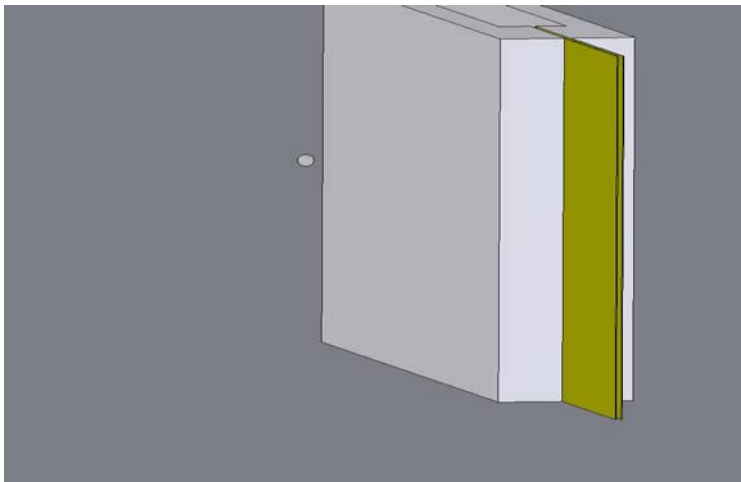
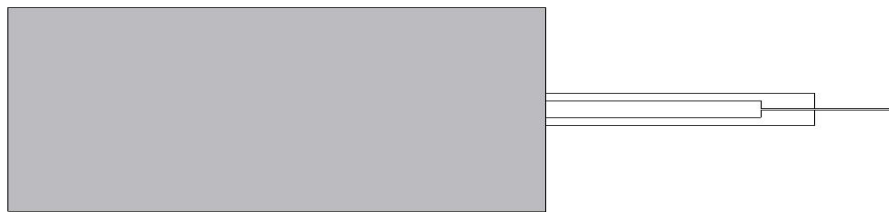
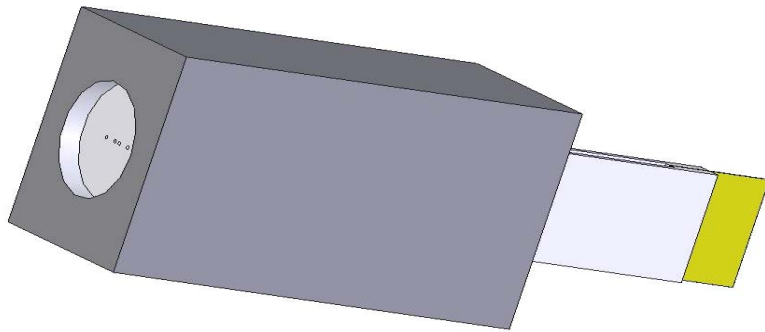


Fig. 31 continued

The first image shows the isometric view of the microgripper attachment designed. The wires are attached to the sample (in gold) for actuation purposes. The second image shows the back side of the gripper that will fit in directly to the BiSlide microassembly system described before. The third image gives a top view of the novel hand design for the gripper and the final image shows a zoomed in view of the PVDF sample attached to the hand that can be actuated for the working of the mechanism. Figure 32 gives a line drawing of the same attachment with the dimensions coming in from the BiSlide system mating parts. The holes at the back enable easy fitting of the attachment on the microassembly. The hands and the body of the attachment are desired to be made of a lightweight material like aluminum.

Figure 32 shows a line diagram of the design. This can be used directly for manufacturing a prototype which is one of the potential future work for this project.

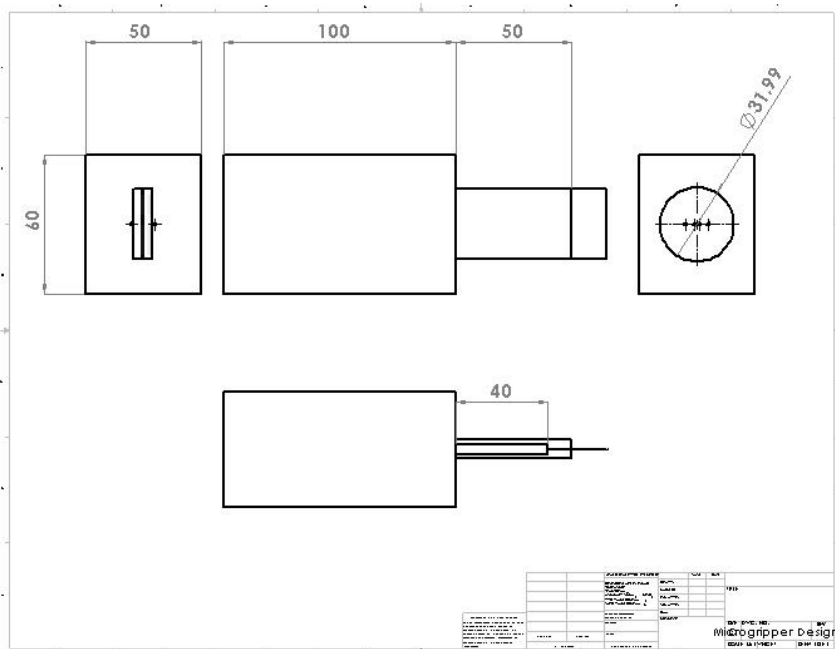


Fig. 32 Line diagram of the microgripper attachment

5. DISCUSSIONS

In this section discussions on results are included in order to obtain scientific understanding. The fundamentally interesting phenomenon we discovered lies in the tribological characterization of the PVDF. The surface characterization furthers our understanding of mechanisms of piezoelectricity.

5.1 Frictional Behavior

This session focuses on the tribological behavior of PVDF as a polymer. Results will be compared with previously published results on other polymeric materials. In such, no piezoelectricity is discussed here.

Previous work has reported that there are several factors dominating frictional behavior of polymers. They are, for example, chain length, crosslinking, adhesion and plastic deformation, among others [67, 68].

The friction characterization of the samples is done as described in the section 3 and the results of these tests are shown in section 4. The friction test data were shown in figures 23 to 26. The friction coefficient is a function of test conditions. The tests with the variation in the speed and the applied load against the coefficient of friction are done in order to calibrate our system and ensure the compatibility with expected results. The basis for performing these tests is to rule out external forces and factors on the tribological characterization of the sample. With the increase of speed, the friction decreased slightly following a linear relationship. Similarly to the applied load, the friction coefficient increases linearly. Comparing with published data, our tests results follow the Amontons' Laws of friction [66].

Our tribological characterization investigates the PVDF-PVDF interaction by sliding. The consideration to be noted is that the polymer that is substituted on the pin is not

electroded and does not have any charge flowing through it. Hence the piezoelectric property of that particular interface is one sided from the sample being tested. For polymeric materials in general the deformation component plays a dominant role in the total friction force [69]. Adhesion is also a factor to be considered for polymer-polymer interaction leading to friction as is the case here. Research has shown that the friction of crosslinked polymers was orders of magnitude greater than that of the uncrosslinked ones [68]. Here since PVDF does not exist in a crosslinked state we can eliminate this factor. Previous work has also shown that the adhesion hysteresis and friction forces increase substantially with increase in the chain lengths [67]. Also the same work showed new ways for manipulating the adhesion and friction of polymer surfaces by adjusting the state of the surface chains [67]. These are interesting follow up works that can yield to further understanding of the problem.

Kaneko [68] showed that the microwear mechanism of polymers must be analyzed from their surface properties, not from their bulk properties, because surface properties are not always identical to the ones expected from bulk materials. The report also showed importantly that during load based friction and wear tests on polymers, the scanning-scratched surfaces formed projections, and no depressions or wear particles were observed as in the case of ceramics [68]. We expect a similar behavior in the case of our sample also.

Another important reference that must be mentioned is the work done by Lavielle [70] on polymer-polymer interaction. This work shows the interference of interfacial and mechanical properties in polymer-polymer tribology. In this work, the friction coefficient μ at equilibrium is shown to be proportional to the corresponding adhesion energy of the same films on a rigid substrate.

5.2 Effects of Surface Roughness on Friction

Surface roughness of a material surface plays an important role in its friction characteristics. The rougher a sample surface is, the more its friction will be. This section discusses the role played by the surface roughness of the PVDF in the observed behavior during its tribological characterization. Previous reports in similar areas are briefed here.

The comparison between samples A and B, which differed mainly in that one was tested parallel to the stretching direction and one perpendicular to it, respectively, shows that the initial value at zero voltage was higher for sample B. The average surface roughness of samples A is 0.374 μm and B 0.486 μm . The average surface roughness measured under an applied voltage of these samples does not change. This means that the surface roughness of piezomaterial does not change due to its piezoelectricity.

In light of this conclusion, we studied the effect of applied potential on the PVDF film thickness. The AFM test shows the increase in thickness for the piezoelectric polymer. No change is found for the unpoled samples.

In terms of friction, the reason sample B has a higher initial value is due to the fact that the surface roughness of B is higher than that of A. It is noticed that the motion of friction is perpendicular to the stretch marks. At non-zero voltage, the value of μ was comparable for both samples, possibly indicating that the effect of voltage on the friction response of both piezoelectric samples was dominant over the initial surface features. The comparison between samples A and B that have similar frictional behavior makes this evident. It is accepted that the surface roughness and elastic modulus affect the friction of polymers [69]. However, our results have shown that the piezoelectricity does not affect surface roughness. Instead, the thickness changes under an applied voltage.

Friedrich [71] described the effects of microstructure in polymer composites on friction and wear properties. They propose models relating the microstructural and mechanical properties of the material to the tribological properties.

The surface roughness tests yield important results as they help us eliminate causes for the observed phenomenon. The dimensional changes in the sample are of the order of nanometers and hence the surface profilometer which gives an output in microns does not yield the profile picture accurately.

5.3 Piezoelectricity Dominated Frictional Behavior

The previous two sections in this section discussed about the various factors that influence the frictional behavior of a PVDF material. In this session, we discuss about the effects of applied potential on friction.

As noted that three samples were tested in this work. The difference between the samples A, B and C is that the first two (A and B) are piezoelectric while the last one (C) is not. This enables us to study the effects of piezoelectricity.

As shown in figures 25 and 26, the friction was “turned on” while the applied voltage was applied. Similarly, when the applied voltage was turned off, the friction was reduced. Such a friction turned “on-off” is an interesting behavior that has not been reported before. Such phenomenon, however, was not observed in the non piezoelectric sample C.

Poled PVDF has a global nonzero polarization P . The polarization P is along the direction of dipole alignment. When voltage is applied across the sample, the dipoles try to rotate and expand or contract in the direction of applied field. The electromechanical expansion or contraction is quantified by the piezoelectric coefficient d_{33} of PVDF, with the strain being a product of d_{33} and the electric field applied [72]. In the case of PVDF,

d_{33} is negative, meaning the sample contracts under positive field and expands under negative field. Similarly, the sample contracts when the polarization P and the field are pointed in the same direction, and it expands when they are in opposite directions. Interestingly, the tests we conducted with inverting voltage and inverting sample polarization with respect to applied voltage confirm that the direction of polarization P with respect to applied electric field plays a role in determining the coefficient of friction. From all these tests and analysis, we have proven that there exists a direct link between the piezoelectric nature of PVDF and its friction response. The direct comparison between samples A and C confirms this conclusion.

Furthermore, looking at the friction response as a function of voltage, from figures 25 and 26, a clear trend emerges. The voltage appears to have an “on-off” effect on the coefficient of friction. The value of friction increases substantially with the application of any voltage but does not vary appreciably with increment in voltage after this. In other words, it is more or less the same with increase in voltage once the voltage is applied. Sample C is not poled and hence the dipoles do not get affected by application of voltage. This sample does not show any marked change in the μ value once voltage is applied. This clearly reiterates the role of the dipoles in affecting the friction.

Inversion of voltage similarly does not affect the coefficient of friction of sample C; although it does in the poled samples. The second experiment shows that the original inversion had the positive polarity of PVDF on its top. Thus when voltage is applied the dipoles aligned such that the negative charge goes towards the top.

Another possible aspect to be considered is the blocked force of the PVDF. Blocked force, refers to the force exerted at a given voltage level when the actuator is constrained from motion. This means that the blocked force can add up to the normal force, and thereby having a direct influence on the friction. However, a previous report [73] ruled this out as the blocked force for PVDF is in the order of a few mN on the application of

around 100 V DC. At the level of voltages we are applying, it is an order of magnitude smaller than that. We do not expect that such a small force would affect the coefficient of friction.

There were reports on electric field and friction. Seto [74] had investigated the effects of an electric field on the static friction of a piezoelectric material. He applied an AC voltage and observed that the friction increased as the frequency of the applied voltage increased. The mechanisms were not discussed in this report.

5.4 Effects of Stress on Piezoelectricity

Since the date of piezoelectricity was discovered, stress is the source to generate electrical output [4]. In the following, we firstly make a brief review of the mechanics aspects of the piezoelectricity. More details are discussed with the effect of a Hertzian contact stress on piezoelectric behavior. There are inconsistent reports that under a Hertzian stress field, the coefficient of friction of certain polymers have been found to vary [75].

As shown earlier, the piezoelectricity is a stress related function [4].

$$d = \left(\frac{\partial D}{\partial X} \right)_{E=0}$$

$$g = \left(\frac{\partial E}{\partial X} \right)_{D=0}$$

$$d = \left(\frac{\partial D}{\partial x} \right)_{E=0}$$

$$h = \left(\frac{\partial E}{\partial x} \right)_{D=0}$$

where X is the stress, x is the mechanical strain, E is the electric field and D is the electric displacement. d, g and h are the coefficients. This indicates that within a unit cell, the output electrical charge is related to the stress and strain.

In the present research, the contact stress is through sliding thus it is non-uniform and non-static. It is necessary to visit the stress distribution according to the Hertzian contact theory [76]. Hertzian contact stress refers to the localized stresses that develop as two curved surfaces come in contact and deform slightly under the imposed loads. In sliding conditions, the stress distribution is illustrated in the Figure 33. Here the contours are of the principal shear stress beneath a sliding contact. This amount of deformation is dependent on the elasticity of the material in contact. In the case of a Hertzian Point contact, there is a direct relation between the applied load and the deformation obtained. In our case, the top layer of PVDF rubbing on the sample is in reality slightly curved as it is fitted to the pin which is curved.

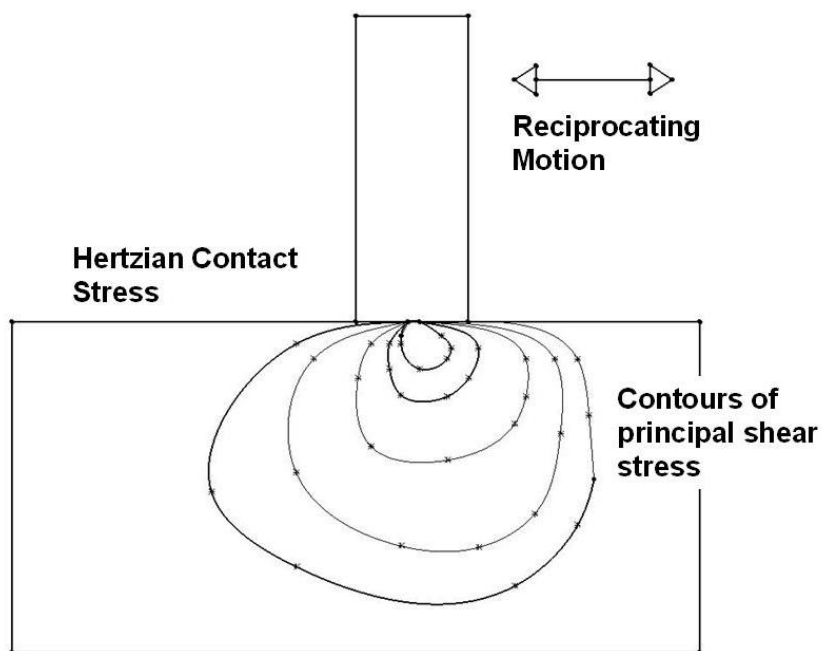


Fig. 33 Hertzian contact stress [77]

It has been reported that in polymers, under the influence of a Hertzian stress field, the friction coefficient decreases with the increase in the contact stress. A report by Wang et al. [75] showed that for a given applied load, increasing the contact stress decreased both the coefficient of friction and the wear rate, with both these factors being interrelated.

This work proposed a function between the coefficient of friction and the contact stress. The authors proposed using their discovery for other semicrystalline polymers in the case of dry sliding similar to ours. Domineci et al. [78] detected shear stress in an elastic layer of PVDF. They used the PVDF as a sensor to resolve the shear stress component. They compare the axi-symmetry elastic problem theory to the response produced by the piezoelectric material and find the response to be the same. The reported approach related the shear stress and the piezoelectricity that was proven to be effective.

Although the Hertzian contact discusses about the Von Misses stress being used for predicting the onset of plastic deformation, the stress distribution under sliding contact indicates the nature of localized stress, particularly with existence of friction.

The effects of microstructure of PVDF on piezoelectricity were analyzed using an AFM, as shown in Figure 28 and 29. We can clearly see the microstructural changes in the material and the expansion of the dipoles that is observed in this regard.

The overall piezoelectric effect is affected by the stress. The tribological investigation presented in this opens new areas of future research which will be discussed in detail in section 6.

5.5 Actuation Tests

The actuation experiments were designed in order to optimize the configuration of the PVDF as a microgripper. The two configurations of a basic unimorph and a bimorph are characterized for their deflection curves and compared with the theoretical curve of deflection versus applied voltage for the PVDF. The actuation curves help us to compare the deflection characteristics of the two basic configurations. There has been extensive research done on the actuator configurations [79, 80]. The effort in this research is taken in order to optimize the performance of a microgripper. Thus, a brief review of the previously done work is provided here.

Recently, novel piezoelectric bending actuators like RAINBOW, CERAMBOW, CRESCENT, d_{33} bimorph and THUNDER have been developed [79]. Kugel et al. [79] conducted a comparative experimental investigation of electromechanical characteristics of these devices along with conventional d_{31} bimorph and unimorph actuators. The important result from the work was that it described a decrease in the mechanical quality factor and resonant frequency of bending vibrations in the unimorph, with increasing electric field is much smaller than that in bimorph actuators. The dependence of the behavior of these devices on the operating conditions governs the selection of a particular device for a specific application [79].

Another report by Kugel et al. [81] showed that a bimorph configuration consisting of piezoelectric segments bonded by a polymeric agent had superior piezoelectric characteristics compared to the unimorphs. Piezoelectric coefficients, electrical admittance, mechanical compliance, and losses of the actuator were found to increase with increasing driving electric field.

Yoshikawa et al. [80] compared unimorph and bimorph actuators and the effects of thermally induced stress on the configuration. Bimorph actuators were found to be significantly more energy efficient than unimorph actuators.

As discussed before, the important consideration for the tests described is the deflection for the configuration of PVDF that would yield better deflection characteristics for lesser applied voltage. Hence from the obtained results, the application demands a bimorph configuration for the PVDF actuator.

5.6 Microgripper Design

The primary goal, as described in Section 2, is to incorporate the scientific findings of the research work into a practical application of a microgripper. The aim is to build a microgripper attachment that has the tactile fingers as the PVDF material and that can be

attached to an existing microassembly for manipulation in the various axes. The gap between the hands of the attachment should be of the order of the actuation of the PVDF at normal voltage levels.

Our design works at optimizing this and uses PVDF as an actuator. Some of the salient features of the microgripper design include its immovable L shaped hands with the PVDF fingers attached on the hands act as fingers for gripping. Some important factors considered in the design stage were the provision of channels for attaching wires to the PVDF material on either side for actuation by application of an external voltage. Insulation has to be provided at the connection of the electroded PVDF and the metallic hand to prevent build up of charge in the segment. The design ensures compatibility with the standard microassembly described before and enables easy working of the system to get the desired action of object manipulation in the microscale.

6. CONCLUSIONS

6.1 Summary

Research was conducted on effects of piezoelectricity on tribological and surface properties of a PVDF material as an actuator. A series of laboratory experiments and surface characterization were carried out in order to optimize the microgripper design and obtain basic understanding of the piezoelectricity.

Results have shown the dependence of the friction characteristics of PVDF to an applied potential. It was seen that the friction can be turned on and off by changing the applied electrical potential.

Fundamentals of friction were studied. The dipole alignment has shown visible influence on friction. Results have shown the thickness change, due to applied potential, that is responsible for friction. Other evidence has shown that the change of directions of microstructure does not show visible effects on friction coefficient. Both samples A and B were in β phases; however, their directions are different in reference to friction direction. This indicates that the frictional behavior is mainly based on the elastic properties that are the same for both samples.

Surface characterization by using an AFM and a profilometer showed that the PVDF materials expanded under the applied electrical potential. The expansion, however, did not show visible effects of surface roughness in a macroscale. However, microscopically, the thickness of the PVDF was increased.

A detailed description of the application with a design based on a commercially available microassembly is shown. Possible manufacturing for a prototype is the next

step. This work attempts to partly succeed in bringing out the true sense of engineering in that it applies science directly to possible application.

Overall, this work opens new areas of fundamental investigation of friction. It linked for the first time the relation between the piezoelectric nature of the materials investigated to the frictional behavior under the influence of an external electric field.

6.2 Suggested Future Research

Future investigation will focus on the nature of dipole structures. This includes applying an alternating current (AC) field on the sample and extending the range of voltage to higher magnitudes. Work can also be done on other polymers of similar configuration and structure such as polyethylene to Teflon by varying the number of fluorine atoms in the sample to study the effects due to fluorine.

Actuation tests can focus on other configurations in order to obtain maximum efficiency for a given applied potential. Manufacturing a prototype will lead to interesting possibilities.

Correlating the frictional behavior of the sample to the piezoelectric nature can be performed for other similar polymers and the phenomenon can yield invaluable information.

Performing a stress based mathematical approach to the problem will yield important understanding of the problem. Detailed analysis will help us correlate the mechanical properties to the behavior better.

REFERENCES

- 1) Ikeda, T., 1990, *Fundamentals of Piezoelectricity*, Oxford University Press, Oxford, UK.
- 2) Cady, W.G., 1964, *Piezoelectricity: An Introduction to the Theory and Applications of Electromechanical Phenomena in Crystals, New rev. ed., 2 vols.* Dover, New York.
- 3) Gaultschi, G., 2002, *Piezoelectric Sensorics*, Springer, Berlin.
- 4) Taylor, G.W., Gagnepain, J.J., Meeker, T.R., Nakamura, T., and Shuvalov, L.A., 1985, *Piezoelectricity*, Gordon and Breach Science Publishers, New York.
- 5) Pauliat, G., Mathey, P., and Roosen, G., 1991, "Influence of piezoelectricity on the photorefractive effect," *J. Opt. Soc. Am.* **B-8**, pp. 1942-1946.
- 6) Furukawa, T., Ishida, K., and Fukada E., 1979, "Piezoelectric properties in the composite systems of polymers and PZT ceramic," *J. Appl. Phys.*, **50**, pp. 4904-4912.
- 7) Kawai, H., 1969, "The piezoelectricity of poly(vinylidene fluoride)," *Japan J. App. Phys.*, **8**, pp. 975-976.
- 8) Bergman, J.G., McFee, J.H., and Crane, G.R., 1971, "Pyroelectricity and Optical second harmonic generation in polyvinylidene fluoride films," *Appl. Phys. Lett.*, **18**, pp. 203-203.
- 9) Nakamura, K., and Wada, Y., 1971, "Piezoelectricity, pyroelectricity, and the electrostriction constant of poly(vinylidene fluoride)," *J. Polym. Sci.*, **A-29**, pp. 161-173.
- 10) Barsky M. F., Lindner D. K., and Claus R.O., 1989, "Robot gripper control system using PVDF piezoelectric sensors," *IEEE Transactions on Ultrasonics, Ferroelectrics, and Frequency Control*, **36(1)**, pp. 129-134.
- 11) Kim, D-H., Kim, B., Kang, H., 2004, "Development of a piezoelectric polymer-based sensorized microgripper for microassembly and micromanipulation," *Microsystem Technologies*, **10**, pp. 275-280.

- 12) Singh, J., 2005, *Smart Electronic Materials*, Cambridge University Press, Cambridge, UK.
- 13) Arnau, A., 2004, *Piezoelectric Transducers and Applications*, Springer, Berlin.
- 14) Yoo, M., Frank, C., Mori, S., Yamaguchi, S., 2004, "Interaction of poly(vinylidene fluoride) with graphite particles: 2. effect of solvent evaporation kinetics and chemical properties of PVDF on the surface morphology of a composite film and its relation to electrochemical performance," *Chem.Mater.*, **16**, pp.1945-1953.
- 15) Park, S-E., and Shrout, T.R., 1997, "Ultrahigh strain and piezoelectric behavior in relaxor based ferroelectric single crystals," *J. Appl. Phys.*, **82**(4), pp. 1804-1811.
- 16) Chen, Q.X., and Payne, P.A., 1995, "Industrial applications of piezoelectric polymer transducers," *Meas. Sci. Technol.*, **6**, pp. 249-267.
- 17) Wang, T.T., Herbert, J.M., and Glass, A.M., 1988, *The Applications of Ferroelectric Polymer*, Blackie, New York.
- 18) Smith, W.A., Shaulov, A., and Auld, B.A., 1985, "Tailoring the properties of composite piezoelectric materials for medical ultrasonic transducers," 1985 Proc. IEEE Ultrasonics Symposium, San Francisco, pp. 642-647.
- 19) Wang, G-F., Yu, S-W., Feng, X-Q., 2004, "A piezoelectric constitutive theory with rotation gradient effects," *European J. Mech.*, **A-23**, pp. 455-466.
- 20) Harrison, J.S., and Ounaies, Z., 2001, "Piezoelectric polymers," *Encyclopedia of Smart Materials*, John Wiley and Sons, New York.
- 21) Kepler, R.G., and Anderson, R.A., 1978, "Ferroelectricity in polyvinylidene fluoride," *J. Appl. Phys.*, **49**(3), pp. 1232-1235.
- 22) Pantelis, P., 1984, "Properties and applications of piezoelectric polymers," *Phys. in Tech.*, **15**, pp. 239-243.
- 23) Broadhurst, M.G., and Davis, G.T., 1980, "*Electrets*," *G.M. Sessler, ed.*, Springer-Verlag, New York.

- 24) Sessler, G.M., 1981, "Piezoelectricity in polyvinylidene fluoride," *J. Acoust. Soc. Am.*, **70**(6), pp. 1596-1608.
- 25) Lovinger, A.J., 1983, "Ferroelectric polymers," *Science*, **220**(4602), pp. 1115-1121.
- 26) Schwartz, M., 2002, *Encyclopedia of Smart Materials*, John Wiley and Sons, New York.
- 27) Polyvinylidene fluoride, Materials Safety Data Sheet (MSDS), 2002, Arkema Inc., Philadelphia.
- 28) Hasegawa, R., Takahashi, Y., Chatani, Y., and Tadakoro, H., 1972, "Crystal structures of three crystalline forms of poly(vinylidene fluoride)," *Polym. J.*, **2**, pp. 600-610.
- 29) Bernholc, J., Nakhmanson, S., Nardelli, M., and Meunier, V., 2004, "Understanding and enhancing polarization in complex materials," *Computing in Science and Engineering*, **6**(6), pp. 12-21.
- 30) Salimi, A., Yousefi, A.A., 2004, "Conformational changes and phase transformation mechanisms in PVDF solution-cast films," *J. Polym. Sci.*, **B-42**, pp. 3487-3495.
- 31) Gregorio, R., Cestari, M.J., 1994, "Effect of crystallization temperature on the crystalline phase content and morphology of poly(vinylidene fluoride)," *J. Polym. Sci.*, **B-32**, pp. 859-870.
- 32) Grubb, D.T., Choi, K., 1981, "The annealing of solution grown crystals of alpha and gamma poly(vinylidene fluoride)," *J. Appl. Phys.*, **52**, pp. 5908-5915.
- 33) Tashiro, K., Tadokoro, H., Kobayashi, M., 1981, "Structure and piezoelectricity of poly(vinylidene fluoride)," *Ferroelectrics*, **32**, p. 167-175.
- 34) O'Connor, D.J., Sexton, B., Roger, C., 2003, *Smart Surface Analysis Methods in Materials Science*, Springer, Berlin.
- 35) Perez, R., Ounaies, Z., 2006, "AFM characterization of electroactive polymer nanocomposites," *Proc. Mater. Res. Soc. Symp.*, **889**, Warrendale, PA.

- 36) Jager, E., Smela, E., and Inganäs, O., 2000, "Microfabricating conjugated polymer actuators," *Science* 24, **290**(5496), pp. 1540 - 1545.
- 37) Hackl, C.M., Tang, H-Y., Lorentz, R., Turng, L-S., and Schroder, D., 2005, "A Multidomain Model of Planar Electro-Active Polymer Actuators," *IEEE Transactions on Industry Applications*, **41**(5), pp. 553-562.
- 38) Smela, E., 2003, "Conjugated polymer actuators for biomedical application," *Advanced Matls.*, **15**(6), pp. 481-494.
- 39) Fu, Y., Harvey, E.C., Ghantasala, M.K., and Spinks, M., 2006, "Design, fabrication and testing of piezoelectric polymer PVDF microactuators," *Smart Mater. Struct.*, **15**, pp. 141-146.
- 40) Bohannan, G., Schmidt, V.H., Brandt, D., and Mooibroek, M., 1999, "Piezoelectric polymer actuators for active vibration isolation in space applications," *Ferroelectrics*, **224**, pp. 211-217.
- 41) Yamakita, M., Kamamichi, N., Kaneda, Y., Asaka, K., and Luo, Z., 2004, "Development of an artificial muscle linear actuator using ionic polymer–metal composites," *Advanced Robotics*, Springer, **18**(4), pp. 383-399.
- 42) Bar-Cohen Y, 2001, "Electroactive polymers as artificial muscles – reality and challenges," *Proc. AIAA Structures, Structural Dynamics, and Materials Conference*, **1492**, Seattle, WA.
- 43) Lee, C.S., Joo, J., Han, S., and Koh, S.K., 2005, "An approach to durable PVDF cantilevers with highly conducting PEDOT/PSS (DMSO) electrodes," *Sensors and Actuators*, **A-121**, pp. 373–381.
- 44) Yamato, H., Kai, K-I., Ohwa, M. Wernet, W., and Matsumurab, M., 1997, "Mechanical, electrochemical and optical properties of poly(3,4ethylenedioxythiophene)/sulfatedpolyβ-hydroxyethers) composite films," *Electrochimica Acta.*, **42**(16), pp. 2511-2523.
- 45) Vinogradov, A.M., Schmidt, H.V., Tuthill, G.F., Bohannan, G.W., 2004, "Damping and electromechanical energy losses in the piezoelectric polymer PVDF," *Mechanics of Matls.*, **36**, pp. 1007–1016.

- 46) Paquette, J.W., Kim, K.J., and Kim, D., 2005, "Low temperature characteristics of ionic polymer-metal composite actuators," *Sensors and Actuators*, **A-118**, pp. 135-143.
- 47) Dargahi, J., Parameswaran, M., and Payandeh, S., 2000, "A micromachined piezoelectric tactile sensor for an endoscopic grasper-theory, fabrication and experiments," *J. Microelectromechanical Sys.*, **9**(3), pp. 329-335.
- 48) Sitti, M., Horiguchi, S., and Hashimoto, H., 1999, "Tele-touch feedback of surface at the micro/nano scale: modeling and experiments," *Proceedings of 1999 IEEE/RSJ International Conference Robotics and Systems*, **2**, pp. 882-888.
- 49) Kim, D-H., Lee, M-G., Kim, B., and Shim, J-H., 2004, "A superelastic alloy microgripper with embedded electromagnetic actuators and piezoelectric sensors," *Proceedings of SPIE*, **5604**, pp. 230-237.
- 50) Park, J., Kim, S., Kim, D-H., Kim, B., Kwon, S-J., Park, J-O., and Lee, K-I., 2005, "Identification and control of a sensorized microgripper for micromanipulation," *IEEE/ASME Transactions on Mechatronics*, **10**(5), pp. 601-606.
- 51) Rossi, D., Lazzeri, D., Domenici, L., Nannini, C., and Basser, P., 1989, "Tactile sensing by an electromechanochemical skin," *Sensors and Actuators*, **17**, pp.107-111.
- 52) Cadoret, G., Smith, A.M, 1996, "Friction, not texture, dictates grip forces used during object manipulation," *J. Neurophys.*, **75**(5), pp. 1963-1969.
- 53) *Friction*, Wear Tribometer CSM Instruments, Manual, CSM Instruments, CA.
- 54) Magonov, S. N., and Heaton, M. G., 2001, "Applications of AFM for polymers," Veeco metrology group, Santa Barbara, CA.
- 55) James, P. J., Antognozzi, M., Tamayo, J., McMaster, T. J., Newton, J. M. and Miles, M. J., 2001, "Interpretation of contrast in tapping mode AFM and shear force microscopy. A study of nafion," *Langmuir*, **17**, pp. 349-360.
- 56) Kalinin, S.V., Karapetian, E., Kachanov, M., 2004, "Nanoelectromechanics of piezoresponse force microscopy," *Phys. Rev.*, **B-70**, pp. 184101 1-24.

- 57) Alexe, M., Gruverman, A., 2004, *Nanoscale Characterisation of Ferroelectric Materials - Scanning Probe Microscopy Approach*, Springer, Berlin.
- 58) Microphotonics Inc., *TR 200 Surface Profilometer Manual*, Irvine, CA.
- 59) Davis, A.F., Nevill, G.E., 1983, "Corrugated PVDF bimorphs as tactile sensors and micro-actuators - A research note," *Robotica*, **1**, pp. 239-240.
- 60) Velmex Corp., *BISLIDE Microassembly Manual*, Bloomfield, NY.
- 61) Hougham, G., Cassidy, P.E., Johns, K., and Davidson, T., 1999, *Fluoropolymers I: Synthesis*, Kluwer Academic/ Plenum Publishers, New York.
- 62) McKinney, J.E., Davis, G.T., and Broadhurst, M.G, 1980, *J. Appl. Phys.*, **51**, pp. 1676
- 63) Anagnostopoulos, J., and Bergeles, G., 2001, "Corona discharge simulation in wire-duct electrostatic precipitator," *J. Electrostatics*, **54**(2), pp. 129-147.
- 64) Jee, T., Mika, B., Lee, H., and Liang, H., 2006, "Effects of microstructures of PVDF on surface adhesive forces," *Tri. Lett.*, Accepted.
- 65) Anatech Corp., *Hummer Sputter Coater Manual*, San Diego, CA.
- 66) Landman, U., Gao, J., Luedtke, W.D., Gourdon, D., Ruths, M., Israelachvili, J.N., 2004, "Frictional forces and Amontons' law: From the molecular to the macroscopic scale" *J. Phys. Chem. B.*, **108**(11), pp. 3410-3425.
- 67) Maeda, N., Chen, N., Tirrell, M., and Israelachvili, J., 2002, "Adhesion and friction mechanisms of polymer-on-polymer surfaces," *Science* **19**, **297**(5580), pp. 379-382.
- 68) Hamadat, E., and Kaneko, R., 1992, "Microdistortion of polymer surfaces by friction," *J. Phys., D: Appl. Phys.*, **25**, pp. A53-A56.
- 69) Bartenev, G.M., Lavrentev, V.V., 1981, *Friction and Wear of Polymers*, Tribology Series 6, Elsevier, New York.
- 70) Lavielle, L., 1991, "Polymer-polymer friction: relation to adhesion," *Wear* (Switzerland), **151**(1), pp. 63-75.
- 71) Friedrich, K., 1986, "Friction and wear of polymer composites," *Z. Werkstofftech.*, **17**(12), pp. 434-443.

- 72) Schaffner, F., Jungnickel, B-J., 1994, "The electric moment contribution to the piezoelectricity of PVDF", IEEE Transactions on Dielectrics and Electrical Insulation, **1**(4), pp. 553-562.
- 73) IEEE Standard on Piezoelectricity, 1987, IEEE Standard 176-1987, 54 pages.
- 74) Seto, T., 1995, "Effects of an electric field on the static friction of a metal on a ferroelectric material," Appl. Phys. Lett., **67**(3), pp. 442-443.
- 75) Wang, A., Essner, A., and Klien, R., 2001, "Effect of contact stress on friction and wear of ultra-high molecular weight polyethylene in total hip replacement," Proc. Instn Mech Engrs, **215**, Part H, pp. 133-139.
- 76) Hertz, H., 1882, "On the contact of elastic solids," J. reine und angewandte Mathematik, **92**, pp. 156-171.
- 77) Johnson, K.L., reprint 2004, *Contact Mechanics*, Cambridge University Press, Cambridge, UK.
- 78) Domenici, C., De Rossi, D., Bacci, A., and Bennati, S., 1989, "Shear stress detection in an elastic layer by a piezoelectric polymer tactile sensor," IEEE Transactions on Electrical Insulation, **24**(6), pp.1077-1081.
- 79) Kugel, V. D., Chandran, S., Cross, L.E., 1997, "Comparative analysis of piezoelectric bending-mode actuators," Proc. SPIE, Smart Structures and Materials 1997: Smart Materials Technologies, **3040**, pp. 70-80.
- 80) Yoshikawa, S., Saarmaa, E., Kottenstette, N., Robert, J., 1998, "Unimorph and bimorph actuators," J. Acoust., **104**(3), pp.1828-1834.
- 81) Kugel, V. D., Chandran, S., Cross, L.E., 1996, "Caterpillar-type piezoelectric d33 bimorph transducer," Am. Inst.of Phys., **69**(14), pp. 2021-2023.

VITA

Saikumar Mani was born in Mumbai, India. His family transferred to Chennai, India where he was raised and schooled. He studied at the P.S Senior Secondary School, one of the city's premier institutions where right from a young age the emphasis was on personal development and importance of education. He did his undergraduate studies at Hindustan College of Engineering, affiliated with Anna University, one of the nation's largest open universities. He pursued a degree in Mechanical Engineering and received his Bachelor of Engineering degree with distinction in 2005. It was here that he was inspired to pursue further studies by encouragement and support from his family and peers. He was very interested in the materials science and engineering field and wanted to pursue research interests in this area. He moved to the United States in 2005 to pursue his master's in Mechanical Engineering at the Texas A&M University, a pioneer in imparting quality education. He finished his master's studies at Texas A&M University in May 2007. He worked in the Surface Science Laboratory under the guidance of Dr. Hong Liang. His focus area of interest is in piezoelectric polymers and their tribological characterization. He has also worked for some time with metals and nanoalloys. He was part of a team which rebuilt a high temperature tribometer setup. Saikumar is the author of one journal paper, accepted by ASME Journal of Tribology, and one conference paper presented at the Joint Tribology Conference.

Saikumar's permanent home address is:

B-15, Pragati Apartments,
19, Lock Street, Kotturpuram,
Chennai – 600028
India